ONE – DIMENSIONAL COMPUTATIONAL FLOW MODELLING USING PATIENT SPECIFIC GEOMETRY TO ASSESS FRACTIONAL FLOW RESERVE (FFR)

DR KEVIN R MOHEE MBChB MRCP(UK)

University of Swansea Medical School

Submitted for the degree of MSc by Research

June 2021

Student number [redacted]

TABLE OF CONTENTS

ACKNOWLEDGEMENTS

I would like to start by thanking Professor Julian P Halcox for welcoming me when I first came to Swansea. Through his guidance and his continuous support, I embarked on this project and I learnt a great deal of cardiology and research from him.

I would also like to Professor Nithiarasu for his help throughout the project.

My special thanks also go to Dr Daniel R Obaid who has continuously encouraged, motivated and guided me from the planning stage of this project until the end.

My heartfelt thanks also go to Dr Jonathan Mynard who allowed me to use his code, guided me through using it during our very early skype conversations all the way from Swansea to Melbourne.

Last but not least, I would like to thanks my parents, Somdeo Mohee and Rojeetah Mohee for their love and continuously supporting me in everything that I undertake.

ABSTRACT

Fractional flow reserve (FFR) improves the assessment of the physiological significance of coronary lesions compared with conventional angiography. However, it requires additional interventional techniques and equipment to perform. Multiple proposed virtual functional indices are derived from coronary imaging alone but require complex computational fluid dynamics modelling which is time-consuming and hence cannot influence immediate clinical management.

The Zienkiewicz Centre for Computational Engineering at Swansea University has developed a reduced order one-dimensional model that generates a “virtual” value of FFR in considerably less time but its accuracy is unknown and has not been validated against invasive FFR. This MSc by research project aims to refine this 1D model with patient specific data and use it to predict the severity of blood flow reduction caused by individual plaques. Clinical data obtained from coronary angiography will be used and patient-specific data will be generated and then validated by already measured invasive derived FFR data. The study will cover blood flow modelling in different arterial network and assess fractional flow reserve (a physiological index determined from the ratio of the pressure distal to a stenosis relative to that before the stenosis).

THESIS OVERVIEW

Chapter 1 In the first chapter, the evidence for the use of FFR for the physiological assessment of myocardial ischaemia will be reviewed particularly focussing on the recent virtual indices of FFR.

Chapter 2 In this chapter, the concept of 1D FFR in one vessel will be introduced and described as a diagnostic modality and a verification study will be performed.

Chapter 3 Describes a refined concept of 1D FFR as applied to a virtual patient with four coronary arteries and a verification study will be performed.

Chapter 4 In this chapter, the validation of 1D virtual FFR against FFR obtained invasively during routine coronary angiography in a cohort of patients assessed for stable coronary artery disease will be assessed.

Chapter 5 Describes the correlation of 1D virtual FFR combined with a novel "functional jeopardy score", BCIS jeopardy score which is a measure of anatomical ischemic burden with the invasively obtained FFR

Chapter 6 Summarises the findings of this work and gives an outlook on future projects.

Chapter 7 Conclusion

LIST OF FIGURES AND TABLES

Chapter 2

Chapter 3

Chapter 4

Chapter 5

PAPER AND ABSTRACT

PUBLICATION

Mohee K, Mynard JP, Dhunnoo G, et al. Diagnostic performance of virtual fractional flow reserve derived from routine coronary angiography using segmentation free reduced order (1-dimensional) flow modelling. *JRSM Cardiovascular Disease*. January 2020.

ABSTRACT

Mohee K, Mynard J, Dhunnoo G*, et al*. Diagnostic performance of virtual fractional flow reserve derived from routine coronary angiography using segmentation free reduced order (1- dimensional) flow modelling *Heart* 2020;106:A30.

List of abbreviations used and definitions of important terms

1D- one dimensional

1D-vFFR- one dimensional virtual fractional flow reserve

ACS- acute coronary syndrome

AUC- area under the curve

CAD- coronary artery disease

CABG- coronary artery bypass grafting

CFD- computational fluid dynamics

CFR- coronary flow reserve

LCX- left circumflex artery

ESC- European Society of Cardiology

FFR- fractional flow reserve

BCIS- British Cardiovascular Interventional Society

BSA- body surface area

CTCA- Computed Tomographic Coronary Angiography

DES- drug eluting stent

DJS- Duke Jeopardy Score

DS- diameter of stenosed lumen

FD-OCT- frequency domain optical coherence tomography

HDM- high-dimensional models

iFR- instantaneous flow reserve

LAD- left anterior descending artery

LDM- low dimensional models

LL- lesion length

LMS- left main stem artery

MACE- major adverse cardiac events

MI- myocardial infarction

MLA- mean luminal area

MLD- mean luminal diameter

OCT- optical coherence tomography

PCI- Percutaneous coronary angioplasty

Pd- Pressure distal to the stenosis

Pa- Pressure proximal to the stenosis

QCA- quantitative coronary angiography

RCA- right coronary artery

SCAI- Society of Cardiovascular Angiography and Intervention

vFAI- virtual functional assessment index

vFFR- virtual FFR

CFR - the ratio of the maximum blood flow achievable under the maximum stress or demand to the blood flow in the basal metabolic state in normal conditions.

True positive (TP) = the number of cases correctly identified as patient

False positive (FP) = the number of cases incorrectly identified as patient

True negative (TN) = the number of cases correctly identified as healthy

False negative (FN) = the number of cases incorrectly identified as healthy

Accuracy: The accuracy of a test is its ability to differentiate the patient and healthy cases correctly. To estimate the accuracy of a test, we should calculate the proportion of true positive and true negative in all evaluated cases.

Sensitivity: The sensitivity of a test is its ability to determine the patient cases correctly. To estimate it, we should calculate the proportion of true positive in patient cases.

Specificity: The specificity of a test is its ability to determine the healthy cases correctly. To estimate it, we should calculate the proportion of true negative in healthy cases.

CHAPTER 1 Background

Introduction

Coronary artery disease (CAD) is one of the leading causes of mortality and morbidity in the Western world and accounts for 17% of all deaths worldwide (1). The manifestation of chest pain, usually indicative of myocardial ischemia, is a useful predictor of adverse clinical outcomes (2, 3). Invasive coronary angiography with its high spatial and temporal resolution has revolutionised the cardiologist's ability to diagnose CAD, making it the gold standard diagnostic and risk-stratification tool of CAD. Nevertheless, this technique has certain limitations, particularly in determining the clinical relevance of an intermediate coronary lesion (diameter of stenosis measuring 40-70%). Previous studies have shown that prediction of ischemia due to intermediate coronary lesions is poor when based solely on angiography (4-6). Hence, sensor guidewire-based techniques such as fractional flow reserve (FFR) have been devised to assess more reliably the functional significance of intermediate coronary lesions by measuring coronary pressure and flow, and are well established in clinical practice (6-8).

This chapter will examine the latest developments in virtual fractional flow reserve (FFR) introducing novel methods of measuring FFR using image based modelling and computational flow dynamics.

Definition of FFR

FFR is defined as the ratio of maximal achievable coronary blood flow through a stenotic vessel to the maximal achievable coronary blood flow in the same vessel without any stenosis. It is calculated using a pressure ratio of pressure measured distal to the stenosis (Pd) and pressure proximal to the blockage (Pa). Pressure distal is measured with a guide catheter during maximum hyperaemic flow, usually achieved after bolus infusion of a pharmacological agent such as adenosine (9-12). Maximal hyperemia is key to adequately assess FFR, because suboptimal microcirculatory vasodilation might underestimate of the functional assessment of coronary stenoses.

Coronary pressure is measured by using a standard 0.014-inch angioplasty guidewire with a high accuracy pressure transducer distal to the coronary stenosis similar to passing a guidewire for attempting percutaneous coronary intervention (PCI) (9). Hence, FFR measurement is usually performed by interventional cardiologists. If PCI is needed as a result of the FFR measurement, the pressure wire can be utilized for stent delivery. The accuracy of FFR as an index of myocardial ischemia has been validated by numerous studies (13-16). In a vessel without any stenoses, the value of FFR is 1. Based on FAME I and FAME II trials (17, 18), lesions with FFR ≤ 0.80 are considered significant and may benefit from coronary revascularization while patients with FFR > 0.80 do not require any coronary intervention. Instead, these patients have excellent prognosis solely based on medical therapy (19).

iFR

iFR is a newer adenosine-independent index of stenosis severity used by operators who are concerned with cost, duration of procedure or side-effects particularly in

asthmatic patients (20). To obtain iFR, the same pressure wires utilized for FFR are passed to a point distal to a stenotic lesion. During a period of diastole known as the "wave-free period," iFR is calculated as the ratio of Pd to Pa. Clinically, iFR may be utilized to assess indeterminate coronary artery stenosis further, for lesions anywhere from 40 to 90%, but recommendations do not include patients with ACS (21). In patients with clinical symptoms or non-invasive testing consistent with ischemia and IFR of 0.89 or less is a candidate for PCI. In a 2017 study, iFR and FFR demonstrated no significant differences in the prediction of myocardial ischemia (22). Götberg et al, in the iFR-SWEDHEART study, further endorsed iFR-guided revascularization as it was deemed non-inferior to FFR-guided revascularization for major adverse cardiac events at 1-year follow-up (23).

Rationale of FFR

Coronary revascularization is frequently performed in a number of patients with angiographically defined stenosis without any clear evidence that their symptoms stem from that coronary stenosis. Many of these patients can be effectively treated with optimal medical therapy as demonstrated by the Clinical Outcomes Utilizing Revascularization and Aggressive Drug Evaluation (COURAGE) trial, the first to compare contemporary medical therapy with contemporary revascularization techniques (24). Coronary angiography also often over-estimates stenoses severity while under-estimating lesion length (24-28). Furthermore, conventional angiography is unable to differentiate ischemia-inducing lesions from haemodynamically non-significant stenoses (29, 30), for this an assessment of the functional significance of

the lesion is required in addition to the anatomical severity which is where FFR has a role.

Features of FFR

Key benefits of FFR include its ease of use and ability to act as an accurate decision-making tool in clinical practice (31, 32). Unlike various other indices, FFR has an absolute normal value of 1 for every patient and every coronary artery (33, 34). FFR is not influenced by variation in blood pressure, heart rate or contractility (35). FFR measurements are extremely reproducible, unrivalled by any other cardiovascular diagnostic tool (36). FFR can potentially be extrapolated to calculate distinct myocardial coronary collateral perfusion and by performing hyperaemic pressure pullback recording elaborate spatial information about the distribution of lesions along the coronary tree (33).

FFR has been validated against a true gold standard in a prospective multi-testing Bayesian approach and is the only physiological measurement to have been validated in such a way (31, 33). FFR has been shown to improve outcome, decrease mortality and reduce costs (37, 40).

Guidelines on FFR

Several major guidelines recommend measurement of FFR as a decision-making tool before considering PCI in patients with stable CAD (38). The European Society of Cardiology guideline has upgraded FFR to a class I-A indication for identifying hemodynamically significant coronary lesions when non-invasive evidence of myocardial ischemia is unavailable (39). Guidelines from the American College of Cardiology issued in 2021 recommend FFR or iFR use for assessing patients with angiographically intermediate stenoses (37, 40).

Clinical use of FFR worldwide

FFR guided PCI improves patient outcomes, reduces the number of stent insertions and lowers the costs of treatment (13). However, even in the USA and many European countries where FFR use is highest, it is used in <12% of PCI procedures and in fewer diagnostic cases (42, 43).

Orvin et al. (43) and Curzen et al. (28) demonstrated the decision of the operator to insert a stent was contrary with FFR measurements in less than 20% of cases. However, it is important to note that 83% of patients in the study had acute coronary syndrome (ACS) in which the clinical applicability of FFR is less established than in patients with stable CAD (44). Hannawi et al (45) carried out a nationwide online survey of current use of FFR among members of the Society of Cardiovascular Angiography and Intervention (SCAI), who by definition have completed at least one full year (or its equivalent) of training exclusively in cardiac catheterization and angiographic techniques and who, after training, have spent a significant percentage of their practice time performing and interpreting cardiac catheterization and angiographic studies. Of 253 members who responded to the survey out of 3,474 members, 145 operators measured FFR in less than one third of their angiograms while 39 never measured FFR (45).

In a 2018 audit carried out by the British Cardiovascular Interventional Society (BCIS), it was reported that FFR was used in <12% of cases, with 13,421 FFR measurements during diagnostic angiography procedures, and 9455 during PCI procedures with a significant variation among centres (42). Measurement of FFR is already part of the pathway in some centres when there is uncertainty about the significance of stenosis from non-invasive imaging.

Reasons for the infrequent use of FFR measurement

Multiple reasons account for the low use of FFR despite a strong evidence base. These include decision making regarding mode of revascularization at time of coronary angiography by PCI operators reserved only to have the competence and facilities to perform FFR. Also, the perception that doing an FFR will prolong the duration of procedure with many operators remaining confident that visual assessment is very accurate and coupled with a myth that multiple visual assessments for instance carried out by numerous cardiologists (invasive and non-invasive and cardiothoracic surgeons) in a “Heart Team” setting improve their accuracy (46).

Virtual FFR

This represents a novel, non-invasive method to assess the FFR of a coronary artery lesion without the practical difficulties that limit invasive techniques. Several groups have used computational fluid dynamics (CFD), image-based modelling coupled with other coronary imaging to calculate FFR without invasive use of a pressure wire and pharmacological agents (46-52).

FFR derived from Computed Tomographic Coronary Angiography (CTCA)

Since the introduction of CTCA in 1998, its use has increased significantly to assess severity of coronary artery stenoses. It is a non-invasive test with a sensitivity of 95% and specificity of 85% to detect significant CAD in patients with stable angina compared to invasive coronary angiography (53, 54). ESC guidelines published in 2019 have given CTCA class IB recommendation as an alternative to coronary angiography to exclude ACS for low to intermediate risk patients with an inconclusive ECG and troponin (55). Factors that make CTCA less attractive include severe calcifications (high calcium score) and elevated or irregular heart rate; and a dearth

of adequate expertise alongside 24 h service that is currently not widely available (53).

Computational modelling- CTCA + CFD

Calculation of FFR from CTCA data has recently emerged as an innovative, non-invasive technique for identifying ischemia inducing stenoses in patients with suspected or known CAD. The procedure employed involves injecting a patient with a contrast material and performing a CT scan. Images obtained from the scanner coupled with CFD are used to determine blood flow throughout the coronary tree and non-invasive computation of FFR (54, 57).

CFD is a branch of fluid mechanics that uses numerical methods coupled with computer algorithms to analyze and model fluid flow. It has a wide spectrum of industrial applications, most well-known is in aeronautics. The basis of all CFD methods is the Navier-Stokes equations for single phase fluid flow (gas or liquid but not both). Usually for predicting fluid flow, a CFD study comprises of 3 stages. Firstly, pre-processing (building of geometry to represent domain of interest), discretizing the domain with meshes and defining the physical model and boundary conditions. Secondly, solving governing equations via numerical solutions and thirdly postprocessing to analyse and present the results (46, 56).

Application of CFD to study coronary blood flow is challenging as the arteries are structures with non-linear elastic properties. However, considerable understanding has been gained on CAD through previous CFD studies (46).

3D computational models derived from CTCA

Studies that have attempted virtual FFR (vFFR) derived from CTCA have gathered the most significant evidence base to date. The DISCOVER-FLOW trial (57) which compared invasive FFR with non-invasive vFFR derived from CTCA showed per-

vessel accuracy, sensitivity and specificity of 84.3%, 87.9% and 82.2% respectively from vFFR derived from CTCA. The performance of vFFR derived from CTCA was superior to CTCA alone for diagnosing lesion stenosis, the latter of which showed an accuracy, sensitivity and specificity of 58.5%, 91.4% and 39.6% (57). The DEFACTO trial, a crucially important multicentre international study compared vFFR derived from CTCA with CTCA for diagnostic accuracy of ischemia. 252 subjects were recruited for which 407 vessels were assessed using FFR. On a per-patient basis, vFFR derived from CTCA was superior to CTCA stenosis for diagnosis of ischemic lesions for accuracy (73% vs 64%), sensitivity (90% vs 84%) and specificity (54% vs 42%). In patients with intermediate stenoses (30-70%), a 2-fold increase in sensitivity was noted from 37 to 82% without any loss of specificity (58). Another study, the ABSORB trial (59) prefers vFFR derived from CTCA as the functional marker to assess coronary stenosis over FFR. vFFR derived from CTCA represents a promising, innovative, non-invasive technology that permits a combination of anatomical and physiological evaluation of CAD that can help patient risk-stratification for invasive angiography and stenting or optimal medical therapy (59).

PLATFORM, a prospective consecutive cohort study was designed to test the hypothesis that patients with suspected CAD investigated using vFFR derived from CTCA guided approach would require fewer invasive angiograms compared to patients who were evaluated based on standard practice. The study included 2 arms: 204 patients underwent elective non-invasive testing and 380 patients underwent invasive testing with diagnostic angiography. In both study groups, subjects were allocated either to usual care or to vFFR derived from CTCA approach. The vFFR derived from CTCA system quantifies FFR using data obtained from a standard CT scan aimed at providing both anatomic data derived from the CT scan and functional

data about any identified ischemic lesions in patients with suspected CAD. Data obtained from the CT scan is forwarded to HeartFlow Inc, a US based medical technology company that uses CTCA, CFD and proprietary software to create a personalized 3D model of the coronary arteries and assess the impact that stenoses have on blood flow by calculating a virtual FFR. The study showed that use of vFFR derived from CTCA resulted in cancellation of 61% of invasive angiographies and doubled the availability of functional data at the time of revascularization (60).

However, the diagnostic accuracy of vFFR derived from CTCA may be affected by various potential limitations such as significant coronary artery calcifications. The use of beta-blockers to reduce heart rate, heart rate variability and use of sublingual nitrates to dilate the coronary arteries have been suggested to minimize artefacts and maximize image quality.

FFR derived from Invasive Coronary Angiography

In 2013, Virtu-1(46), a single centre prospective study in Sheffield used generic boundary conditions for CFD analysis to calculate virtual FFR in 20 patients with CAD undergoing rotational angiography. The 3D computational model used predicted physiologically significant (FFR<0.80) lesions with accuracy, sensitivity and specificity of 97%, 86% and 100% respectively. vFFR values differed from pressure derived FFR by ± 0.06 (mean=0.02, SD=0.08) and vFFR and FFR were closely correlated (r=0.84). Virtu-1 showed that FFR could be reliably predicted without any need for invasive pressure wire measurements or inducing hyperaemia with pharmacological agents. However, Virtu-1 investigated only simple lesions and generation of vFFR values took over 24h (46).

Tu et al (48) elaborated a novel strategy based on 3D Quantitative Coronary Angiography (QCA) and thrombolysis in myocardial infarction (TIMI) frame count. The study reconstructed anatomical models by 3D-QCA, applied CFD using mean volumetric flow rate of hyperaemic derived 3D QCA and TIMI frame count at the boundaries. This technique used FFR at hyperaemia and mean pressure at the guiding catheter tip at inlet instead of using generic boundary conditions. This led to a fast simulation approach. It revealed that there was good correlation ($r=0.81$; $P<0.001$), with a mean difference of $r=0.81$; $P<0.001$ was found between FFR derived from QCA and FFR. FFR derived from QCA had an overall accuracy, sensitivity and specificity of 88%, 78% and 93% respectively (48).

Papafaklis et al. (47) developed a fast but simplified method of virtual assessment of coronary stenosis from routine angiographic data and compared it against pressure wire-FFR. Three-dimensional quantitative coronary angiography (3D-QCA) was performed in 139 vessels (120 patients) with intermediate lesions assessed by wire-FFR (reference standard: ≤0.80). The 3D-QCA models were processed with CFD to calculate the lesion-specific pressure gradient (ΔP) and construct the ΔP-flow curve, from which the virtual functional assessment index (vFAI) was derived. The discriminatory power of vFAI for ischaemia- producing lesions was high (area under the receiver operator characteristic curve [AUC]: 92% [95% CI: 86-96%]). Diagnostic accuracy, sensitivity and specificity for the optimal vFAI cut-point (≤0.82) were 88%, 90% and 86%, respectively. Virtual-FAI demonstrated superior discrimination against 3D-QCA-derived % area stenosis (AUC: 78% [95% CI: 70- 84%]; $p<0.0001$ compared to vFAI). There was a close correlation ($r=0.78$, $p<0.0001$) and agreement of vFAI compared to wire-FFR (mean difference: -0.0039±0.085, $p=0.59$) (61). However, the flow used to calculate the FFR is pre-specified and assumed to be

equal in all stenoses. However, we know from several studies that there is a large variation in hyperaemic blood flow in patients with CAD (62-65). Such oversimplification of baseline flow boundary conditions and hyperaemic response may work on average but can lead to incorrect results and compromise patient safety when applied to individual cases, across a wide spectrum of patient anatomies.

CT angiography has limited spatial resolution compared to invasive coronary angiography which is another limitation. QCA and 3D QCA are subject to movement artefacts and can artificially smooth the artery wall. Loss of high resolution vessel geometry can lead to underestimation of lesion severity and erroneous FFR computation (65).

FFR derived from Optical Coherence Tomography (OCT)

Virtual FFR can also be estimated by frequency domain optical coherence tomography (FD-OCT). This is a high resolution imaging technology based on near infrared light that was originally used to image transparent samples like fibre optics and retina, has been developed for intracoronary imaging, especially identifying vulnerable plaque and guiding coronary interventions (66). Its superior spatial resolution has made it a useful tool for studying acute occlusion with drug eluting stents (DES), investigating potential markers of DES success and identifying plaques that lead to ACS. FD-OCT is another innovative technique for quantitative estimation of stenosis severity. It provides cross-sectional images of coronary arteries and deployed stents with micron resolution and assesses lumen size with excellent reproducibility. Likewise, it provides information about plaque vulnerability, and calcification estimates, blood flow resistance and microvascular resistance of the vessel portions imaged. FFR can be calculated from blood flow resistance and

microvascular resistance using volumetric analysis of FD-OCT images. FD-OCT derived FFR showed significant correlation with pressure derived FFR (67).

Stefano et al. (68) determined the correlation between FFR and OCT derived lumen dimensions in 14 patients with 18 stenoses but no significant correlations between FFR and OCT measured minimum lumen area (MLA) (r=0.167, P=0.56), minimum lumen diameter (MLD) (r=-0.42, P=0.13) and percent area stenosis (%AS) (r=0.29, P=0.29) were found.

Gonzalo et al. (69) assessed the diagnostic accuracy of OCT derived lumen measurements identifying stenosis severity in 56 patients with 61 stenoses and reported poor but significant correlation between FFR and OCT measurements, MLA (r=0.51, P<0.01), MLD (r=0.4, P=0.05) and %AS (r=0.33, P=0.02).

Zafar et al. (70) carried out a pilot study enrolling 20 patients to evaluate the relationship between pressure derived FFR and FFR derived from OCT. A moderate but significant correlation between pressure derived FFR and FFR derived from OCT was detected (r=0.69, P=0.001) and Bland-Altman analysis showed that the mean differences between FFR and FFR derived from OCT were 0.05±0.14 (70).

FD-OCT is a promising tool in assessing stenotic lesions and can evaluate any feature of plaque instability in situations of ACS and negative FFR. With further testing, FFR derived from OCT may become a valuable tool to evaluate coronary artery stenosis and may play a key role in guiding interventional procedural planning and decision making.

Virtual Functional Assessment Index and Virtual Distal Coronary to Aortic Pressure Ratio

Papafaklis et al. (47) developed a simplified approach for virtual functional assessment of coronary stenoses from routine angiographic data using the Caas Workstation Quantitative Coronary Analysis (QCA)-3D from Pie Medical Imaging (Maastricht, the Netherlands) to recreate coronary geometry. Further processing involves steady-flow CFD analysis using flow rates of 1 and 3 ml/s, corresponding to the average flow at rest and during hyperemia. The pressure gradients at these two flow rates were calculated from the difference of the average pressure at the inlet and outlet and a ratio of Pd/Pa was derived. The average computed pressure ratio over this flow range was named the virtual functional assessment index (vFAI). This model was studied retrospectively in a multi-centre cohort of 120 patients and 139 vessels. It demonstrated that, for an optimum vFAI value of 0.82, the ability to discriminate ischaemia-producing lesions was very good with the area under the receiver operating characteristic curve (AUC) 92% (95% CI: [86–96%]), and the correlation with invasive FFR was reasonable (r=0.78). Diagnostic accuracy, sensitivity and specificity were 88%, 90% and 86%, respectively. The virtual resting Pd/Pa with an optimal cut-off ≤0.94 performed less well when correlated to invasive FFR (r=0.69) (47).

A limitation of this system is that the processing was 15 minutes per vessel, which is not ideal for the workflow in a typical catheterisation laboratory. In addition, vFAI is entirely a function of the geometry of the stenosis. It cannot be a surrogate for FFR because FFR is a measure of the pressure gradient in the context of patient-specific, microvascular physiology. It is therefore likely to be less accurate in patients with microvascular disease, scar or increased myocardial mass (47).

Using the same Caas Workstation QCA-3D, Masdjedi et al. (71) have proposed a new method for simulating FFR from conventional angiography. The 3D coronary reconstruction is processed semi-automatically based on two angiographic projections. The boundaries were defined as a constant parabolic flow incorporating the measured aortic pressure at the inlet and stress-free (zero pressure) at the outlet approximating the coronary wall as rigid and the blood as Newtonian fluid. The pressure drop is then calculated based on physical laws incorporating viscous resistance and separation loss effects resulting in a parameter named vessel-FFR (commonly given the acronym vFFR, not to be confused with virtual FFR described previously in (47), which is computed via a different method). This algorithm was then retrospectively applied to a cohort of 100 patients with an intermediate degree of stenosis in the Fast Assessment of STenosis severity (FAST) study that found a good correlation between the offline simulated vessel FFR and invasive FFR ($r=0.89$; $p<0.001$). Bland Altman limits of agreement were impressive at ± 0.03.28 (71).

Conclusion and potential of FFR derived from 1D model

Calculation of FFR derived from CTCA has been carried out so far in a number of studies using 3D models of the coronary tree and ventricular myocardium. The patient anatomy is modelled from a mid-diastolic time point and extracted from semi-automatic data. Since the flow and pressure were unknown a priori, the 3D model needed the blending of lumped parameter models of the microcirculation. These models need to be adjusted so that both the cardiac output and the mean aortic pressure fit with the clinical data. Similarly, FFR derived from rotational coronary angiography and from a 3D model requires 1 day (46). Besides the costs and computation time, another major drawback of the HeartFlow model is that the

software is not in the ambit of the medical research community and cardiac health care providers (57). During the past 2-3 years, there has been a growing interest in using reduced order models for coronary haemodynamics mainly because they are very quick and can easily incorporate relevant anatomical information (72, 73).

Thus, Mynard and Nithiarasu have proposed a more simplistic 1D model with the additional benefit of providing accurate time-dependant information at lower costs and at reduced computation time (74-77). Simulated data from 1D models exhibit many of the characteristics of the systemic and coronary arteries of both normal and pathological physiologic and geometric data. Application of 1D models using conventional diagnostic coronary angiography without the need for segmentation remains relatively new.

CHAPTER 2- Verification study on one coronary artery to assess effect of virtual FFR with increasing length of stenosis and increasing % area of stenosis

Introduction

The cardiovascular system is a complex circulatory system which consists of a muscular pump that beats rhythmically – the heart, a system of tubes - arteries and veins and valves (78). Recently, with advances in computational modelling, simulation of the hemodynamic properties of cardiovascular system has played an increasingly important role in the diagnosis of cardiovascular diseases and the development of medical devices as well as pharmacological agents (79–81).

At present, computational simulation models can be segregated into two types, high-dimensional models (HDM) and low dimensional models (LDM) as described in Figure 2.1 (82).

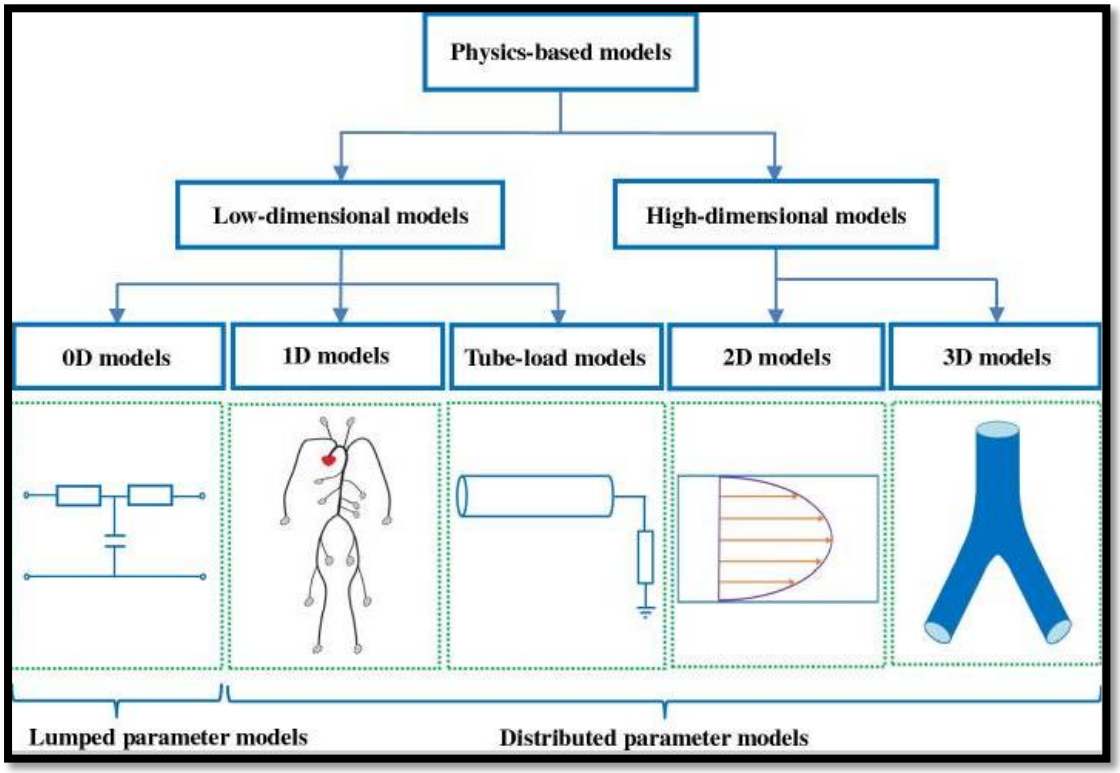

Figure 2.1 Flow diagram of physics-based models in the cardiovascular system (Adapted from Zhou et al, 2019) (82)

HDM consist of 2D models and 3D models that can provide us with an elaborate pictorial representation of the fluid dynamics of blood flow patterns in the cardiovascular system. 2D models are usually applied to describe variations of blood flow around the radius in an axis-symmetric tube representing a coronary artery in this instance (83, 84). 3D fluid-structure interaction models are used to simulate the interaction between fluid (blood) and structure (vessel walls) (85, 86). It is challenging both in terms of resource and time to acquire a 3D model of the whole arterial tree due to difficulty in extracting the precise geometry of vascular structures, hence HDM usually use computational fluid dynamics to simulate pressure variations with varying morphology of the stenoses within specific arterial sites rather than the entire arterial tree.

LDM provides less detail in regard to patient-specific information, but with the advantage of much reduced workload and computational resources. Hence, due to its ability to generate a result within minutes, LDM have great practical feasibility in clinical practice to influence decision-making compared to HDM which require a comparable longer processing time. Currently, LDM mainly consist of 0D models, 1D models and tube-load models.

0D models, also known as lumped parameter models, can indicate global properties of the arterial tree. The lumped parameter models are represented by their pulse waveforms as a function of time only. The most well-known lumped parameter model is the Windkessel model (87), which includes single-compartment models and multi-compartment models (88, 89). 1D models and tube-load models are distributed parameter models, which can represent distributed properties of the arterial system. In the latter two types of models, their pulse waveforms rely on both time and spatial dimension. In the distributed parameter models, 1D model based on the simplified

Navier–Stokes equation is usually applied to represent pressure and flow at any position in the entire arterial tree (82, 90–92). The Windkessel model is computationally simple but lacks precision. The present study utilises 1D modelling to estimate a value of FFR.

Aim

The aim of this study was to perform a verification study on one hypothetical coronary artery of length 10 mm entire vessel segment without any side branches and to assess effect of virtual FFR with:

1) increasing length of stenosis by increment of 10 mm but keeping stenosis constant
2) increasing % area of stenosis by increment of 20 %

Method

The above data was then introduced in a spreadsheet (Appendix) where the areas, wave speeds, and some material properties of the arteries were estimated from the inlet and outlet radii. Additionally, the excel sheet generated a text file with the connectivity of all the arterial network and information about the geometrical and material properties. These areas, material properties, and lengths are the input for a computer code in Matlab that generates the mesh to be introduced in the numerical scheme to compute different physical quantities like length of lesion, inlet and outlet area and resistance. These physical quantities were then used to compute the virtual FFR to predict the CAD severity.

The model uses established methods described extensively previously (93-95). The coronary stenosis was represented with the lumped parameter stenosis model

described by Young and Tsai (95), which contains empirically validated coefficients derived from stenosis length and relative diameter. Based on preliminary studies, the main determinant of FFR in such models is the flow through the stenosis. A representative coronary flow waveform was prescribed at the inlet and the outlet was represented by a two elements Windkessel method (capacitor and resistor) while the patient-specific mean flow passing through the stenosis was estimated as described above.

A coronary artery was represented as a single segment, split into three parts, proximal part, stenosis and distal part, each represented individually as one-dimensional (1D) segments described by the equations of fluid flow and an equation governing the non-linear pressure-area elasticity relation. The proximal and distal segments were 4 cm and 2 cm respectively. The wave speed which determines the stiffness of the segments was fixed at 8 m/s. The lumen shape was assumed as circular and its area was represented by $\pi(C/2)^2$.

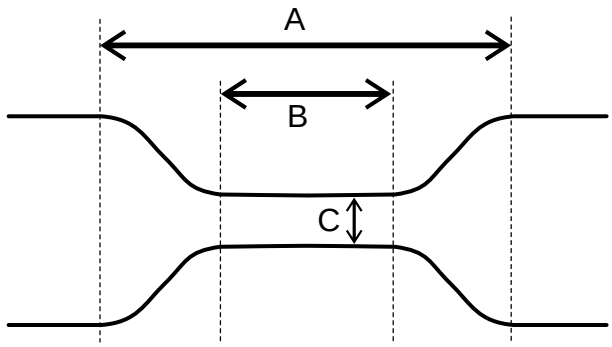

proximal stenosis distal

A= length of coronary vessel under examination

B= length of coronary stenosis (lesion length, LL)

C= diameter of stenosed lumen (mean luminal diameter, MLD)

Figure 2.2 shows typical coronary artery split into proximal, stenosis and distal part

Results

Percentage stenosis increases whilst FFR decreases, most significantly after the 80% stenosis mark. Lower FFR, Mid FFR and High FFR are three constants that were used during the experiment as the flow rate.

Lesion length/mm	% area stenosis	FFR
5	80	0.62
10	80	0.59
15	80	0.55
20	80	0.52
25	80	0.50

Table 2.1- Table showing values of FFR generated with increasing lesion length

Mean luminal diameter/mm	% area stenosis	FFR
3.6	10	0.99
3.2	20	0.99
2.8	30	0.99

2.4	40	0.99
2.0	50	0.98
1.6	60	0.95
1.2	70	0.84
0.8	80	0.34
0.4	90	NA

Table 2.2- Table showing values of FFR generated with increasing % stenosis area

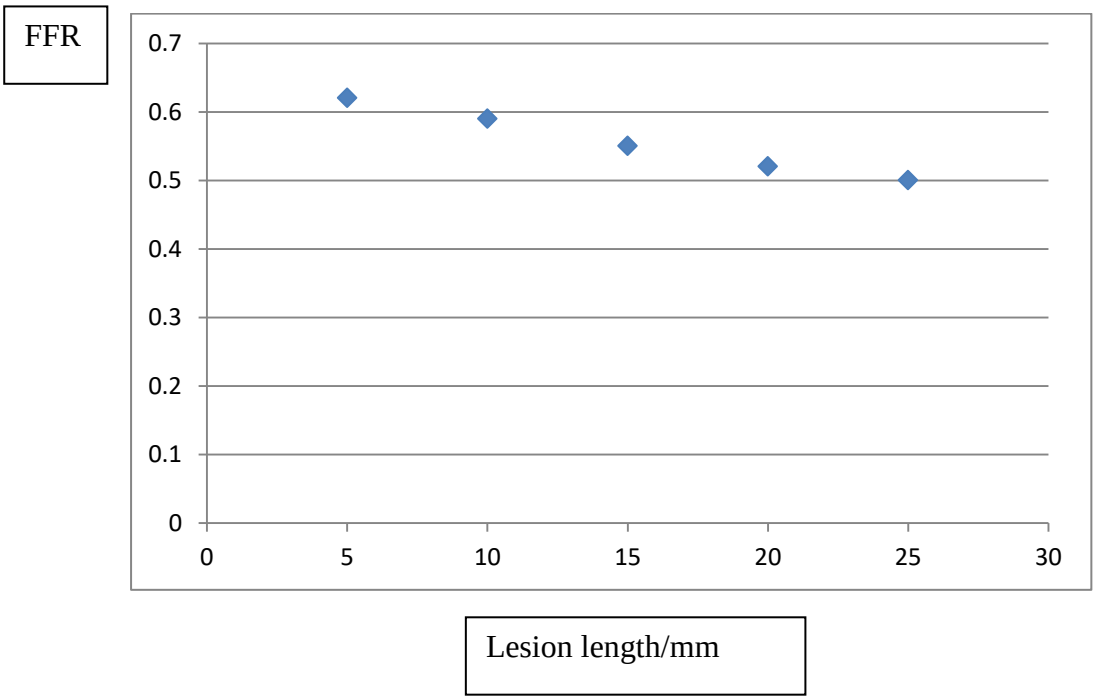

Figure 2.3 Effect of increasing lesion length on FFR

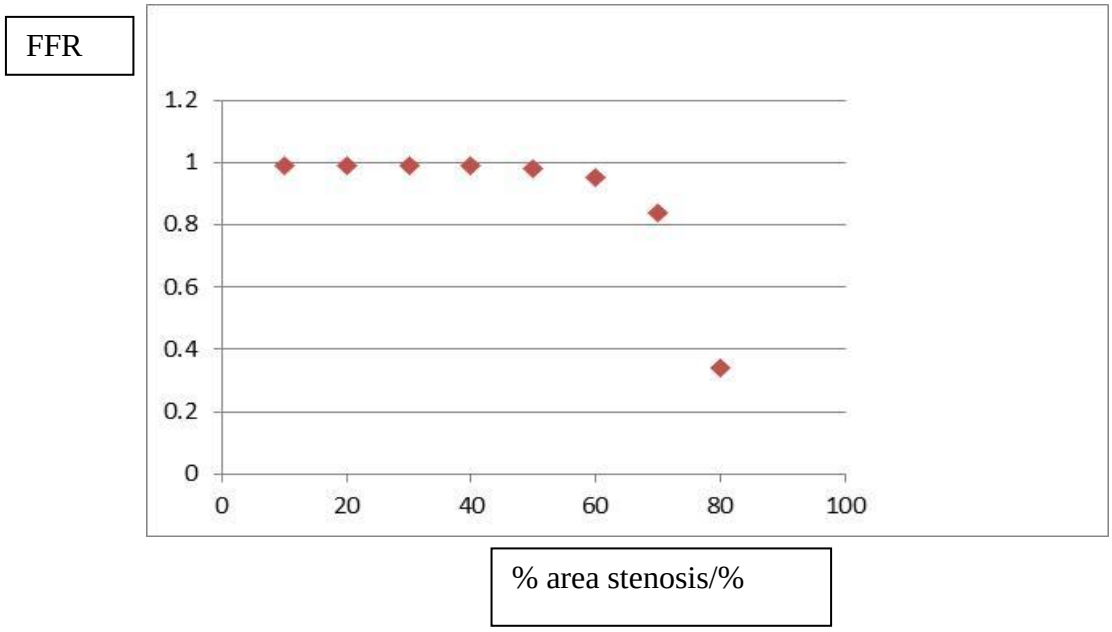

Figure 2.4- Effect of increasing % area of stenosis on FFR

Discussion

This study demonstrates two findings. Firstly, as length of stenosis increases, FFR decreases. Secondly, as % area of stenosis increases, FFR decreases, more markedly at 70% area stenosis when FFR<0.8. However, with high degree of stenosis above 80% stenosis, it has been observed the 1d-vFFR code is unable to generate recordable value. This occurs because velocity becomes very high in the stenotic region. There is a stability condition in the 1D formulation, such that if velocity exceeds the wave speed of the vessel, the numerical will 'blow up' due to a limitation of the numerical scheme used to solve the basic equations. Our study shows a weak inverse linear relationship of increasing lesion length with decreasing FFR as shown previously by Brosch et al. (96) and Alghamdi et al. (97). However, in the presence of a high-grade stenosis (>70% diameter reduction), the effect of the lesion length (LL) is not clinically relevant as compared to the stenosis diameter,

hence a sharp exponential decline in FFR which was observed is similar to Alghamdi et al (97) and Takagi et al (98).

A pursuit for alternative non-invasive assessment of functional significance of coronary stenoses without the need for a pressure-wire has led to the development of new software solutions that allow the construction of a 3-D computational fluid dynamics using the routine CT angiography and invasive coronary angiographic data.

Recently, several research teams have developed systems that derive physiological data from invasive angiographic images resulting in calculation of physiological indices as surrogates of invasively measured FFR with high diagnostic efficiency of this method (46-52). Nevertheless, one of the disadvantages these non-invasive techniques is their high computational complexity, and to assess the non-invasive FFR, time-consuming calculations requiring high computational power. These models also require the input data to be processed manually. All these factors make the implementation of this approach difficult in clinical practice.

Our method allows the calculations to be made even when computing power is limited, as a typical FFR calculation run on a laptop takes no longer than 3 minutes after quantitative coronary angiography (QCA) data has been acquired for length of stenosis, cross-sectional area pre-stenosis location and cross-sectional area at site of stenosis.

Conclusion

Our study has shown promising result in one virtual coronary artery and my next step will be to validate it in the four main coronary arteries.

CHAPTER 3 - Verification study on one hypothetical patient with four coronary arteries using 1D-vFFR

Introduction

In this study, we aim to perform a verification study on one virtual male patient of average height 1.7 m and weight 70 kg.

Method

The height and weight for this hypothetical patient was assumed as 1.7m and 70 kg respectively. To avoid the need for additional invasive measurements a number of assumptions were applied. From the body surface area (BSA), cardiac output was approximated based on three assumed cardiac indices of 2.5 L/min/m^2, 3.0 L/min/m^2 and 3.5 L/min/m^2, derived from healthy subjects >60 years old using cardiac magnetic resonance imaging (99). The coronary flow reserve (CFR) was assumed as 3 based on data in human subjects presenting with chest pain and who had angiographically normal coronary arteries (100). It was assumed that the increase in flow under hyperaemic conditions is proportional to the resting flow, by reducing coronary resistance by a factor of 0.22, corresponding to a 3.5-fold increase in flow with respect to resting conditions (101).

Step 1 **Assumed cardiac index**
CI

Step 2 **Estimate cardiac output via BSA**
BSA
Cardiac output (CO)

Step 3 **Estimate total coronary flow**
Total coronary flow (proportion of CO)
Total coronary flow (absolute)

Step 4 **Estimate hyperaemic flow**
Basal flow x 4.2

Step 5 **Calculate constant multiplier for the code**
Mean flow when the constant is 1
Constant multiplier to input into code

Figure 3.1 shows 5 steps taken to calculate the hyperemic flow for each case

1D Computational flow analysis

The coronary geometrical data consists of data such as lesion length (LL) and minimal lumen diameter (MLD) that were then combined with the estimated patient specific coronary flow rate calculated above and was incorporated into the 1D model containing wave speeds, material properties of the arteries and boundary conditions. The in-house code developed by Swansea University Engineering group then generates the mesh to be introduced for analysis (102). This creates estimates of pressures from which 1D-vFFR can be derived.

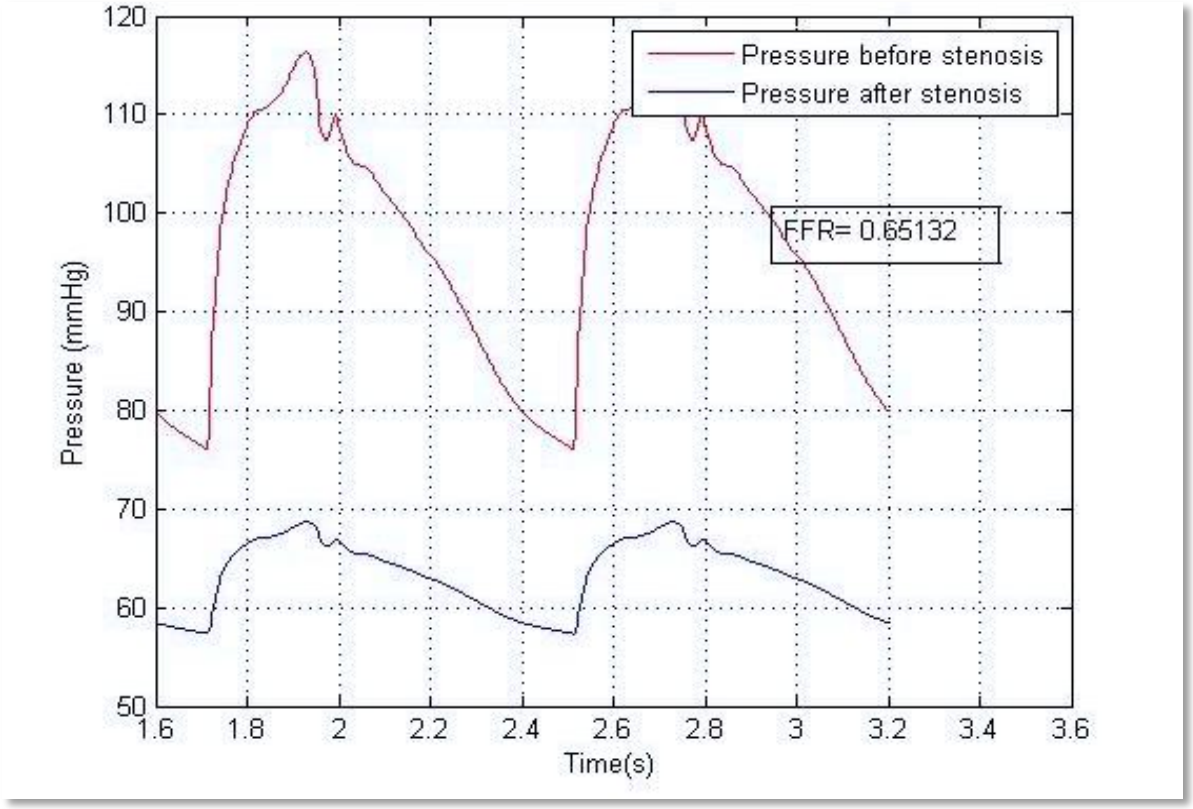

Figure 3.2 shows a typical pressure input for a stenosed artery generated from Matlab

Results

The four coronary arteries left main stem (LMS), left anterior descending (LAD), right coronary artery (RCA) and left circumflex (LCX) with diameters 6 mm, 5 mm, 4 mm, 3 mm respectively were chosen. For each coronary artery, the length of stenosis was increased by 10 mm from an initial value of 10 mm and %area of stenosis increased by 10% from their corresponding initial diameters ie. LMS 6 mm, LAD 5 mm, RCA 4 mm and LCX 3 mm. Three values of FFR were obtained named, lower FFR, mid FFR and high FFR due to three values of cardiac indices used as part of a sensitivity analysis study.

Coronary Artery	Length of coronary artery/mm	Diameter of stenosed lumen	% area stenosis	Lower FFR	Mid FFR	High FFR
RCA	10	3.6	10	0.99	0.99	0.98
	10	3.2	20	0.99	0.99	0.98
	10	2.8	30	0.99	0.99	0.98
	10	2.4	40	0.99	0.98	0.97
	10	2.0	50	0.98	0.97	0.94
	10	1.6	60	0.95	0.93	0.77
	10	1.2	70	0.84	0.68	NA
	10	0.8	80	0.34	NA	NA
	10	0.4	90	NA	NA	NA
	20	3.6	10	0.99	0.99	0.98
	20	3.2	20	0.99	0.98	0.97
	20	2.8	30	0.99	0.98	0.97
	20	2.4	40	0.98	0.97	0.94
	20	2.0	50	0.96	0.94	0.89
	20	1.6	60	0.91	0.86	0.69
	20	1.2	70	0.74	0.59	0.28
	20	0.8	80	0.29	0.15	NA
	20	0.4	90	NA	NA	NA
	30	3.6	10	0.99	0.99	0.98

	30	3.2	20	0.99	0.98	0.97
	30	2.8	30	0.98	0.97	0.96
	30	2.4	40	0.97	0.96	0.93
	30	2.0	50	0.95	0.92	0.85
	30	1.6	60	0.88	0.82	0.64
	30	1.2	70	0.68	0.53	0.26
	30	0.8	80	0.25	0.14	NA
	30	0.4	90	NA	NA	NA

Table 3.1- Variation of FFR with increasing % area of stenosis and lesion length in RCA.

Length of stenosis 10mm

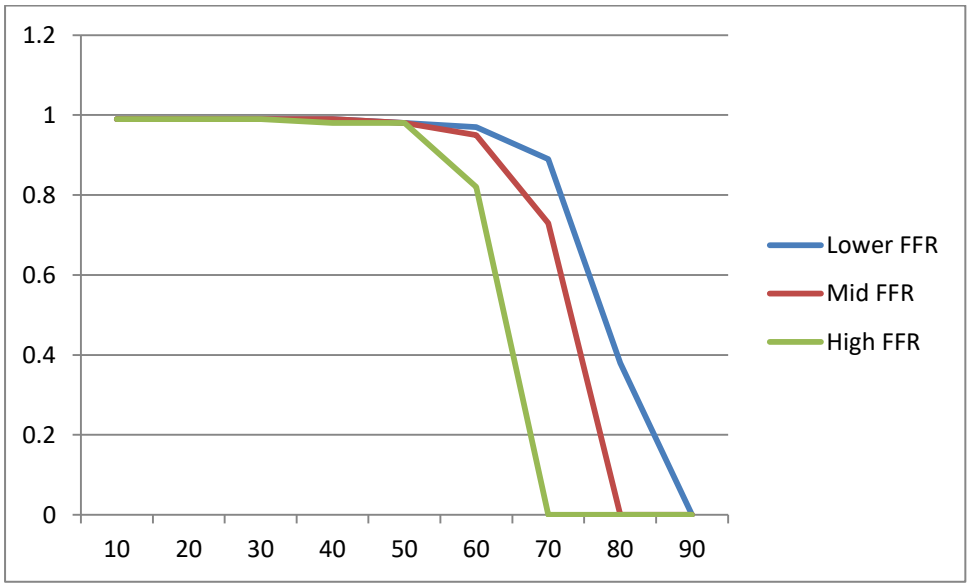

Figure 3.3- Variation of FFR with increasing % area of stenosis with lesion length 10mm in RCA.

Length of stenosis 20mm

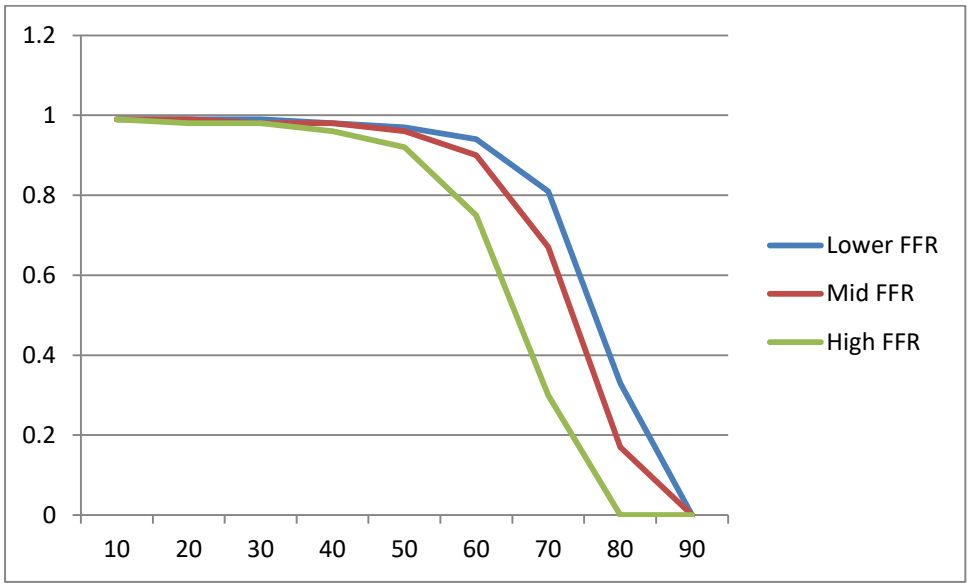

Figure 3.4- Variation of FFR with increasing % area of stenosis with lesion length 20mm in RCA.

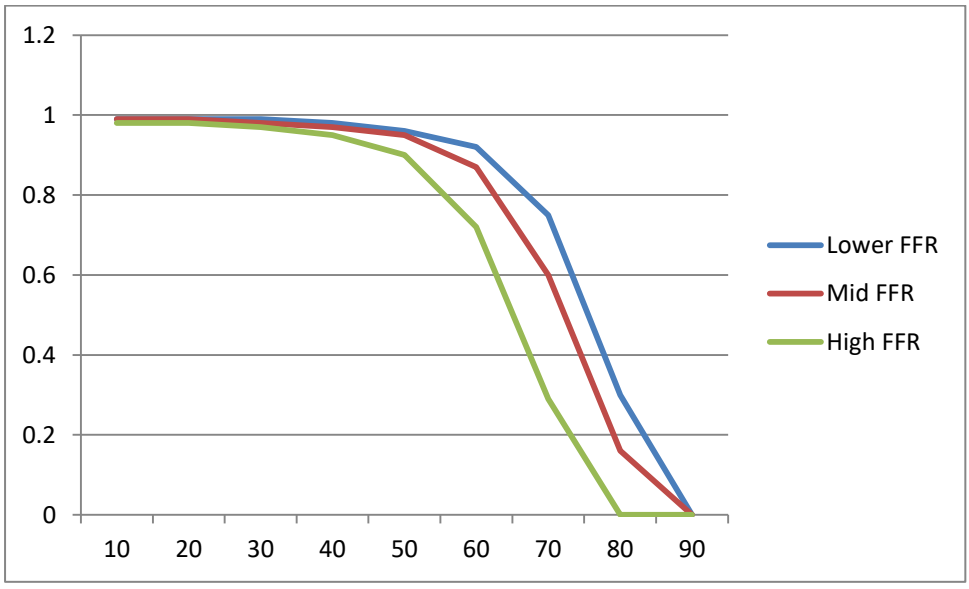

Figure 3.5- Variation of FFR with increasing % area of stenosis with lesion length 30mm in RCA.

Discussion

This study confirms two findings. Firstly, as length of stenosis increases, FFR decreases. Secondly, as % area of stenosis increases, FFR decreases, more markedly at 60% area stenosis when FFR<0.8. However, with high degree of stenosis above 80% stenosis, it has been observed the 1D-vFFR code generates a value of 0.2-0.4 and is sometimes unable to generate recordable value. This may be due to the high coronary flow with the value of cardiac index of 3.5 L/min/m^2. When a cardiac index of 2.3 is used, it has been observed that the 1D-vFFR code generates a value of >0.8 even at % area stenosis of 70%.

Our method allows the generation of a typical FFR calculation run on a laptop and takes less than 3 minutes after acquisition of coronary angiographic data.

Limitations

Numerous limitations need to be accounted for in this study. Lesion irregularity and length, amount of myocardium supplied by the target vessel, the presence of diffuse coronary artery disease and microcirculatory impairment as well as wall deformation, bifurcation and tortuosity are not accounted for in this model (103, 104). In addition, atherosclerotic plaques are complex in shape, and plaque characteristics such as length, shape, irregularity and eccentricity will all contribute to altering the resistance to flow across a coronary lesion and affect FFR. In this study, coronary stenosis was assumed to be symmetrical.

Conclusion

This study shows that FFR value decreases with increasing mean luminal diameter and lesion length. In the next study I plan to validate 1D-vFFR on a cohort of stable coronary artery disease patients who have undergone invasive coronary angiography with FFR and also to address some of the assumptions regarding coronary flow.

CHAPTER 4- Diagnostic Performance of Virtual Fractional Flow Reserve derived from routine Coronary Angiography using Segmentation Free Reduced order (1- Dimensional) Flow Modelling

Background

The accuracy of FFR as an index of myocardial ischemia is validated and widely accepted (13-16). FFR-guided PCI improves patient outcomes, reduces number of stent insertions and lowers cost of treatment (13). However, it is used in <10% of PCI procedures even in the UK (105) and less than 40 % in European countries where the leaders in 2015 were Denmark (31%) and Belgium (29%) (106, 107), likely in part due to the additional time and cost incurred in performing invasive FFR.

Virtual FFR represents a novel, non-invasive method to assess FFR of a coronary artery lesion without the practical difficulties that limit the invasive technique. Recently, several virtual FFR methods have used full 3D segmentation and 3D computational fluid dynamics simulations. These take time, entail significant cost and require expertise in image-based computational fluid dynamics (CFD) coupled with either CT coronary angiograms or invasive rotational coronary angiography to calculate FFR without insertion of a pressure wire or use of pharmacological agents (46, 48, 57, 60, 108). With a view to reducing some of the above constraints, several groups are exploring simpler ‘reduced-order’ virtual FFR methods that involve 1D simulations, but still use a 3D segmentation to generate the 1D geometry (48, 108).

The aim of this chapter is to investigate whether useful virtual FFR results can be obtained with a 1D model using only a few basic measurements of stenosis geometry obtained from routine coronary angiographic images. This will enable fast, low cost and viable results for immediate decision-making in the clinic or catheter laboratory without complex image segmentation or complex CFD software.

Methods

Study Population

In this single centre retrospective study, we included subjects aged ≥18 years who were investigated for chest pain with coronary angiography, and in whom a coronary stenosis was detected and were subsequently investigated with an FFR measurement after obtaining informed consent. Patients with in-stent restenosis at the target vessel, previous bypass surgery, and diffuse coronary disease were excluded.

Coronary Angiography and Invasive FFR measurements

Diagnostic coronary angiography was performed using a 5F or 6F catheter according to local procedures. At least 2 orthogonal projections were acquired of all potential coronary stenosis. After heparin (70–100 IU/kg IV) administration, and intra-coronary nitrate to obtain maximum coronary vasodilatation a calibrated 0.014-inch "PressureWire" guide wire (St Jude Medical, USA) was introduced into the guiding catheter. The pressure wire was advanced into the guiding catheter until the pressure transducer was just outside its tip, and the pressure measured by the sensor was then normalized to that of the guiding catheter. The wire was then advanced into the vessel, distal to the target coronary stenosis. FFR was calculated as the lowest ratio of distal coronary pressure divided by aortic pressure after achievement of maximal hyperaemia at the steady-state, obtained using adenosine administration. Maximal hyperaemia was assumed after at least 1 minute in the presence of stable systemic blood pressure, decreased compared with baseline, remaining for at least 10 beats (13).

Quantitative Coronary Angiography

Quantitative assessment of stenosis severity at coronary angiography was performed offline and independently by two cardiologists using two-dimensional Quantitative Coronary Angiography (QCA) with a computer assisted automatic arterial contour detection system (Centricity CA-1000, GE Healthcare, Little Chalfont, United Kingdom) in the end-diastolic angiographic image, with optimal projection showing minimal foreshortening of the lesion. The software utilizes measurement calibration by comparing it with an object of known dimension and allows rapid quantification of vessel size and lesion length.

The cardiologists were blinded to clinical and hemodynamic data. Pixel size was determined with automated distance calibration and all analyses were performed on frames demonstrating optimal luminal opacification. The proximal and distal limits of the lesion were defined by manual inspection (corresponding to the sites of minimal luminal encroachment i.e., mean 10% diameter decrease compared with the reference vessel). The automated edge-detection software was then used to trace the lesion contours and determined the reference vessel diameter and luminal diameter at maximal obstruction. Reference vessel diameter (RVD), lesion length (LL) and minimal lumen diameter (MLD), and percentage diameter of stenosed lumen (DS) were calculated.

Calculation of 1D FFR:

Patient specific data to calculate an estimate of flow rate

For all patients height and weight were recorded and a value of body surface area (BSA) calculated (109). To avoid the need for additional invasive measurements a number of assumptions were applied. From the BSA, cardiac output was

approximated based on an assumed cardiac index of 3 L/min/m^2, derived from healthy subjects >60 years old using cardiac magnetic resonance imaging (95). A coronary flow reserve of 3 was assumed, based on data in human subjects presenting with chest pain and who had angiographically normal coronary arteries (103). Based on the estimated cardiac output, estimated total coronary blood flow was derived from an assumed myocardial mass based on the relationship between normalized proximal arterial diameters and myocardial mass for different segments of LAD, LCX and RCA (113). Vessel-specific baseline coronary flow was then assumed to be proportional to subtended myocardial mass, based on an allometric scaling principle (113-117). Cross-sectional areas of LCA and RCA were calculated from LCA and RCA measurements, then allometric scaling was carried out by initially calculating flow through the left main coronary artery, assuming flow is divided between LCA and RCA in proportion to their areas. The coronary flow in the stenotic branch was calculated based on the area ratio of the stenotic branch to the left main coronary artery. An estimate of the hyperaemic flow was then derived from which a mean flow rate in the vessel of interest was obtained. We assumed that the increase in flow under hyperaemic conditions is proportional to the resting flow, by reducing coronary resistance by a factor of 0.22, corresponding to a 3.5-fold increase in flow with respect to resting conditions (104).

1D computational flow analysis

The coronary geometrical data was extracted offline from 2-dimensional coronary angiograms using QCA. The extracted data (Reference vessel diameter (RVD), lesion length (LL), minimal lumen diameter (MLD), and percentage diameter of stenosed lumen (DS) was then combined with the estimated patient specific

coronary flow rate calculated above and was incorporated into the 1D model containing wave speeds, material properties of the arteries and boundary conditions. The in-house built code developed by Swansea University Engineering Group then generates the mesh to be introduced for analysis (99). This creates estimates of pressure (PD and PA) from which 1D-vFFR can be derived (Figure 1). The model uses established methods described extensively previously (94-102). The boundary conditions were identical to the one described in Chapter 3.

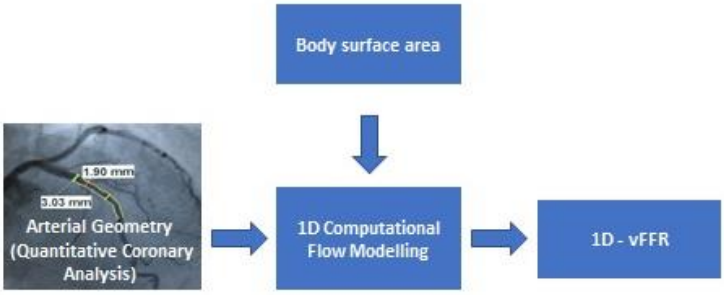

Figure 4.1- Flow diagram showing the steps in creating the 1D-vFFR.

A coronary artery is represented as a single segment, split into three parts, proximal part, stenosis and distal part is represented individually as one-dimensional (1D) segments, described by the equations of fluid flow and an equation governing the non-linear pressure-area elasticity relation. The coronary stenosis was represented with the lumped parameter stenosis model described by Young and Tsai (101), which contains empirically validated coefficients derived from stenosis length and relative diameter. Based on preliminary studies, the main determinant of FFR in such models is the flow through the stenosis. A representative coronary flow waveform was prescribed at the inlet, while the patient-specific mean flow passing through the stenosis was estimated as described above.

Statistical Analysis

Statistical analysis was performed using the Statistical Package for the Social Sciences (SPSS 23.0, IBM Corp., Armonk, New York, USA). The correlation (Pearson) of both 1D-vFFR and QCA were compared to FFR. The diagnostic accuracy of 1D-vFFR was compared with QCA and against pressure-derived FFR using point estimates of sensitivity and specificity, and area under the curve analysis from receiver-operator characteristic curves (ROC). Statistical significance was accepted at a value of $p < 0.05$.

Results

The 85 patients included 62 males with mean age of 64 ± 9 years old. Baseline characteristics of all patients are shown in Table 1. Mean FFR was 0.84 (SD 0.07) and 32% of the stenoses had an FFR value <0.80, and hence underwent revascularization.

Mean Age, years	64(9)
Male, n	62
BMI, kg/m2	28.3(4)
Coronary arteries, n	
RCA	19
PDA	1
LMS	1
LAD	67

LCX	11
D1	1
OM1	2
QCA Mean coronary stenosis area,%	54 (16)
Coronary stenosis diameter/mm	1.31(0.5)
QCA Mean coronary stenosis diameter,%	44(12)
QCA Mean lesion length, mm	13 (7)

Table 4.1- Baseline characteristics of all patients (n=85)

BMI: body mass index, RCA: right coronary artery, PDA: posterior descending artery, LMS: left main stem, LAD: left anterior descending, LCX: left circumflex artery, D1: first diagonal branch, OM1: first obtuse marginal branch, QCA: quantitative coronary angiography.

QCA revealed the mean percentage of coronary stenosis by area was 54% ± 16% and the mean lesion length 13 ± 7 mm. Once angiographic images of the coronary artery had been acquired calculation of the 1D-vFFR took less than 1 minute. Coronary stenosis (QCA) had a statistically significant but weak correlation with FFR (r=-0.2, p= 0.04) and poor diagnostic performance to determine lesions causing significant reductions in FFR (<0.80), (area under the receiver operator characteristic curve (AUC) 0.39, p= 0.09). If a QCA area stenosis of 50% was taken as the cut off the sensitivity to detect a significant stenosis (FFR<0.8) was 58% and the specificity 26%. If a more severe QCA area stenosis of 70% is used, then the sensitivity decreases to 11% with an increase in specificity to 71%. Compared with QCA, 1D-

vFFR had a stronger correlation with FFR (r=0.32, p=0.01). Although the correlation between 1D-vFFR and FFR was only modest, 1D-vFFR provided an improvement in diagnostic accuracy over QCA (Figure 2). Overall compared with QCA, it showed significantly better diagnostic performance (AUC 0.67, p=0.007) (Figure 3). Using a 1D-vFFR cut of 0.7 gave a sensitivity of 92% and a specificity of 29%.

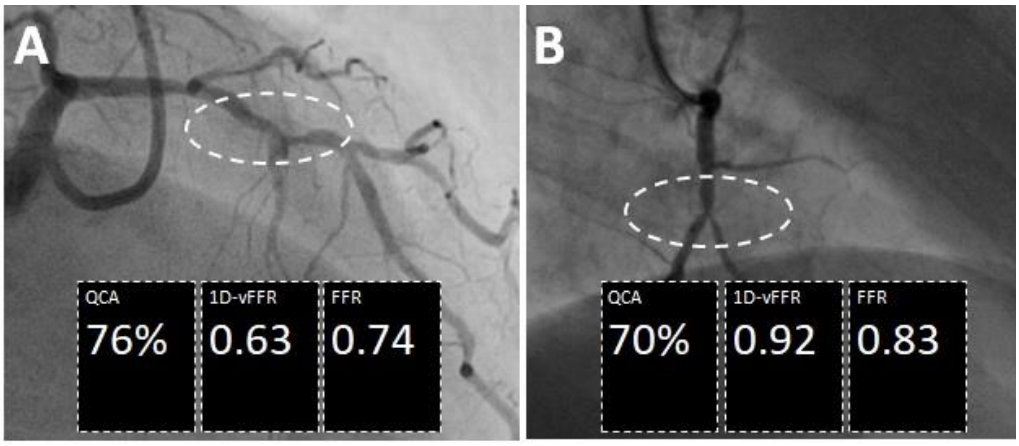

Figure 4.2 (A) Positive stenosis by QCA (>70%) correctly predicts positive FFR (<0.80) with 1D-vFFR also positive (<0.75).

Figure 4.2 (B) Positive stenosis by QCA (>70%) provides a false positive reading as FFR is >0.80, 1D-vFFR (>0.75) correctly predicts lesion in not functionally significant.

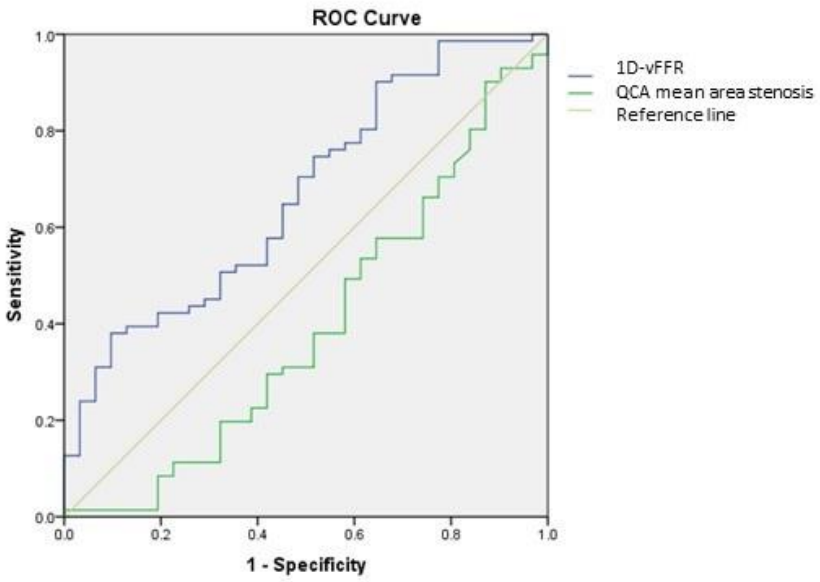

Figure 4.3. Receiver Operator Characteristics (ROC) Curves comparing the diagnostic utility of mean area stenosis (derived from Quantitative Coronary Analysis (QCA)) and 1D-vFFR.

Discussion

QCA vs. 1D-vFFR

We found that QCA was poor at determining a functionally significant stenosis by FFR. A QCA stenosis cutoff of 50% had a sensitivity of only 58% to detect an FFR<0.80, in contrast, if 1D-vFFR was used with a cut off 0.75 then the sensitivity was 83%. If the more stringent 1D-vFFR cut off 0.70 is used, then the sensitivity goes up to 92%, specificity is 29%.

Computational based methods to derive FFR

Calculation of FFR derived from CTCA has been performed for some time using 3D models of the coronary tree and ventricular myocardium modelled from a mid-diastolic time point. The coronary tree is segmented into millions of separate finite

elements and computational flow dynamics used to calculate the pressure loss at specific locations by solving the Navier-Stokes equations. However, this is computationally very demanding requiring export of the images to a specialist facility with a processing time of at least 24 hours. This derived FFR_{CT} (HeartFlowInc, California, US) had a sensitivity of 85% and specificity of 79% in intermediate (30%-70%) stenosis (115). If used as a “gatekeeper” pre catheter lab it has been shown to reduce the number of coronary angiograms showing non-significant disease without impacting on the number requiring PCI (116). FFR_{CT} does have some limitations; numerous artefacts may affect CTCA interpretability including calcification, misalignment, motion, and increased image noise. These may affect the model accuracy, preventing the calculation of an FFR_{CT} in a third of cases in one study (117, 118).

Angiography based methods to derive FFR

Invasive angiography remains the most widely used modality to assess coronary anatomy and numerous methods have been used to attempt to derive a “virtual” FFR from the invasive angiogram. Morris et al described one technique that derives the CT 3D coronary model from angiography rather than CTCA (119). This initially included pulsatile coronary flow which complicates the computation further requiring more than 24 hours to complete, however a later iteration utilising a “pseudo-transient” model of coronary flow reduced this time to <4 minutes but currently requires invasively measured coronary microvascular resistance (120). Both these techniques require rotational angiography which is not widely available and reduces their applicability. Other models use 3D-QCA and simplified computational flow modelling to rapidly derive a virtual FFR (34, 35). The latter, QFFR was recently evaluated in the prospective, multi-centre FAVOR II trial where it demonstrated a

sensitivity of 87% to detect invasive measured FFR positive lesions (50). Although promising, the requirement for 3D QCA, a modality not widely available limits its current utility.

Recently FAVOR III trial which uses Quantitative flow ratio (QFR) to estimate FFR using 3D coronary reconstruction and computational fluid dynamics based on angiography alone showed that based on QFR the revascularisation strategy changed for almost a quarter of patients. QFR calculation was rapid with an average calculation time of 3.9±1.4 minutes and led to reduced numbers of stents implanted, contrast use and radiation exposure along with a shorter procedural time (121).

Potential of reduced order models

Reduced order models for coronary haemodynamics are attractive as they are very quick and can easily incorporate relevant anatomical information. A reduced-order model is used to calculate the pressure and flow distribution for each coronary tree. Subsequently, for each location along the coronary tree, we extract quantitative features describing the anatomy as well as the computed FFR value at that location. They have existed since the 1970s with Young and Tsai (52, 95) able to predict pressure drops within about 20% for a variety of flow conditions and stenosis geometries, including both symmetric and non-symmetric stenosis. Pellicano et al. (122) describe FFR_{angio} which utilises a hybrid reduced order formulation with reduced order modelling of coronary flow in healthy regions and a more complex model in coronary stenosis. In the recent FAST-FFR trial this demonstrated impressive sensitivity (94%) to detect invasive FFR measured coronary stenosis (123). The model only requires standard angiographic images and the computational processing time is less than 3 minutes, however, image segmentation is still required

which is done by specialised software which is then manually corrected, for which the time required is not specified and accounted for as a limitation (123).

In this study we used a 1D model initially described by Mynard and Nithiarasu (124). Application of 1D models to coronary circulation have shown promising results using CTCA (123-125) but to date this study is first to determine FFR from a standard coronary angiogram using a purely 1D model without 3D segmentation.

Limitations

Several limitations should be acknowledged. Our results represent a retrospective, small single centre experience including 102 intermediate coronary stenoses only and hence needs confirmation with larger, prospective multi-centre studies. In addition, patients who had previously undergone revascularization via coronary artery bypass grafting (CABG) surgery or had re-stenosis lesions were excluded from the study; for that reason, the accuracy of 1D-vFFR in these populations remains unknown.

Although at a cut off of 0.75, 1D-vFFR achieved a good sensitivity (83%), good positive predictive value (74.7%) and accuracy (68.6%) it had a low negative predictive value (52.4%) and specificity (35%) which meant a high rate of false positive (64.5%). With a cut off of 0.70, 1D-vFFR showed a higher sensitivity (92%), comparable positive predictive value (74.1%), better accuracy (72%) and negative predictive value (60%), but lower specificity (29%) and higher false positives (71%). This is most likely due to the assumptions that are inevitably required for the

approach that we adopted; for example, improved estimation of hyperaemic coronary blood flow may improve accuracy further. In addition, stenosis geometry was represented by only three parameters (reference vessel diameter, percent stenosis and stenosis length); although missing complex features of the geometry, this approach was intentionally adopted to avoid the complex and time-consuming 3D segmentation process.

Conclusion

1D-vFFR improves the determination of the functional significance of coronary lesions compared with conventional angiography. It is derived using routine angiographic data and does not require a pressure-wire or hyperaemia induction. Standard QCA is used and no specialised image segmentation is required meaning it is fast enough to influence immediate clinical decision making and simple enough to be easily incorporated in the clinical workflow. Whilst the high sensitivity achieved raises the possibility that positive invasive FFR may be predicted in patients with a low 1D-vFFR, future work is required to establish whether this approach could have clinical value.

CHAPTER 5- Validation of virtual FFR derived from routine Coronary Angiography using 1D Flow Modelling and minimal segmentation with the addition of the BCIS jeopardy score

Introduction

FFR guided-revascularisation by percutaneous intervention (PCI) has been associated with a reduction in Major Adverse Cardiac Events (MACE) (14, 15). Functional information on the significance of a coronary artery stenosis as provided by FFR only assesses the presence of ischemia to a certain myocardial territory. However, FFR does not provide any information on the myocardial volume subtended by the stenotic coronary artery. This information is vital as patients with 10-12.5% ischaemic myocardium tend to benefit the most from revascularisation (126).

Hence, several jeopardy scores have been developed and validated (127, 128) to overcome this limitation. A jeopardy score is a simple method for estimating the amount of myocardium at risk on the basis of the particular location of coronary artery stenoses.

These scores are based on the anatomical location and severity of coronary lesions which do not directly incorporate the functional significance of a stenosis. Several of these scores are complex to use, time consuming, have high inter-observer variability and only provide information on risk of the procedure rather than ischaemic burden (129).

Aim

The aim of the current study is to validate the diagnostic performance of a virtual FFR (vFFR) technique using routine angiographic images without any image segmentation (130) combined with a functional jeopardy score such as the BCIS

jeopardy score and a rapidly performed reduced order (one-dimensional) computational model (1D-vFFR).

Methods

The same study population, coronary angiography and invasive measurements and method to calculate 1D-vFFR as described in detail in Chapter 4 was used. Based on the physiological principle that the amount of myocardial mass perfused affects the physiological severity of stenosis the 1D-vFFR was weighted depending on the Myocardial Jeopardy score. The angiographic BCIS-1 Myocardial Jeopardy Score (BCIS JS) (126) was used to classify the extent of coronary artery disease (CAD) due to the fact that the computational model is not equipped with an anatomical functionality as shown in Figure 5.1.

REVIVED **BCIS-1 Jeopardy Score**

	Coronary Artery/Graft	Instructions	Score
1	LMS	if ≥50% lesion, score 8 and go to row 11 if <50% lesion, score 0 and go to row 2	
2	Proximal LAD (Before DG)	if ≥70% lesion, score 6 and go to row 5 if <70% lesion, score 0 and go to row 3	
3	Mid LAD (After DG)	if ≥70% lesion, score 2 and go to row 4 if <70% lesion, score 0 and go to row 4	
4	Major DG	if ≥70% lesion, score 2 and go to row 5 if <70% lesion, score 0 and go to row 5	
5		If Cx dominant, go to row 8 If RCA dominant, go to row 6	
6	Proximal RCA (Before PDA)	if ≥70% lesion, score 4 and go to row 10 if <70% lesion, score 0, go to row 7	
7	PDA	if ≥70% lesion, score 2 and go to row 10 if <70% lesion, score 0, go to row 10	
8	Proximal Cx (Before OM)	if ≥70% lesion, score 6 and go to row 14 if <70% lesion, score 0, go to row 9	
9	Mid Cx (After OM)	if ≥70% lesion, score 2 and go to row 10 if <70% lesion, score 0, go to row 10	
10	Major OM	if ≥70% lesion, score 2 and go to row 14 if <70% lesion, score 0 and go to row 14	
11		If Cx dominant, score 4 and go to row 14 If RCA dominant, score 0 and go to row 12	
12	Proximal RCA (Before PDA)	if ≥70% lesion, score 4 and go to row 14 if <70% lesion, score 0 and go to row 13	
13	PDA	if ≥70% lesion, score 2 and go to row 14 if <70% lesion, score 0, go to row 14	
14		Previous CABG? If yes, go to row 15 If no, go to row 21	
15	LAD graft beyond DG	if <70% graft lesion, score -4, go to row 16 if >70%, poor run-off or n/a, score 0, go to row 16	
16	Major DG graft	if <70% graft lesion, score -2, go to row 17 if ≥70%, poor run-off or n/a, score 0, go to row 17	
17	Major OM graft	if <70% graft lesion, score -2, go to row 18 if ≥70%, poor run-off or n/a, score 0, go to row 18	
18	Cx graft beyond OM (Cx dominant system)	if <70% graft lesion, score -4, go to row 19 if ≥70%, poor run-off or n/a, score 0, go to row 19	
19	RCA graft (before PDA)	if <70% graft lesion, score -4, go to row 21 if ≥70% poor run-off or n/a, score 0, go to row 20	
20	PDA graft	if <70% graft lesion, score -2, go to row 21 if ≥70% poor run-off or n/a, score 0, go to row 21	
21	TOTAL SCORE	Add filled in scores and enter (range: 0 to 12)	

Figure 5.1- BCIS-1 Jeopardy Score

It provides a semi quantitative estimate of the amount of myocardium at risk as a result of severe coronary stenoses (0=no jeopardy; 12=maximum jeopardy). Briefly, the coronary tree was divided into 6 segments: the LAD, diagonal branches of the LAD, septal perforating branches, the circumflex coronary artery, obtuse marginal branches, and the posterior descending coronary artery. Two points were assigned to each of these segments. All segments distal to the index stenosis were considered to be at risk. The maximum possible score is 12 for all myocardial mass

and, for example, 6 for the proximal LAD. The initial 1D-vFFR was weighted according to the myocardial jeopardy score (JS<3 x0.9, JS 3-5x0.95, JS 6-8x1.05, JS 9-12 x1.1) to give the final 1D-vFFR. The benefit of adding the jeopardy score, hence an experimental study was conducted with increasing incremental weighting to assess (if any) any benefit on the 1D-vFFR.

Statistical Analysis

Statistical analysis was performed using the Statistical Package for the Social Sciences (SPSS 23.0, IBM Corp., Armonk, New York, USA). Positive predictive value (PPV), negative predictive value, sensitivity, specificity, and receiver-operator characteristic curves were derived in the usual fashion. Statistical significance was accepted at a value of $p < 0.05$ for primary analyses. Receiver-operating characteristic curve (ROC) area under the curve analysis was undertaken to evaluate the discriminatory ability 1D-vFFR to detect FFR ≤0.8. The correlation of 1D-vFFR was compared to FFR as well as QCA alone with a stenosis of (50%) considered severe.

Results

The 85 patients included 62 males with mean age of 64 ± 9 years old. Baseline characteristics of all patients are shown in Table 1. The three main vessels were uniformly represented. In addition, most of the lesions involved a restricted area of myocardial territory as assessed by the Duke Jeopardy Score (DJS) (DJS=2, 60%). Mean FFR was 0.84 (SD 0.07) with the majority of the stenosis (n = 68, 68%) with an FFR value >0.80, thereby not referred for revascularization.

QCA revealed mean coronary stenosis area was 54% ± 16% and mean lesion length 13 ± 7 mm. Once angiographic analysis of the coronary artery had been performed

calculation of the vFFR took less than 1 minute. Coronary stenosis (QCA) had a statistically significant but weak correlation with FFR (-0.1, p= 0.05) and poor diagnostic performance to determine lesions causing significant reductions in FFR (<0.80), (area under the receiver operator characteristic curve (AUC) 0.67, p= 0.88) sensitivity (stenosis 50%) was 58% and specificity 26%. In contrast, vFFR derived from BCIS- Jeopardy scores had a stronger correlation with FFR (r=0.13, p=0.047) and better diagnostic performance but not statistically significant (AUC 0.60, p=0.12). The sensitivity of vFFR derived from BCIS-JS at BCIS-JS FFR of 0.75 was 87% and specificity 39% whilst 1D vFFR which had a better correlation with FFR ($r = 0.32$, $p = 0.01$) and significantly better diagnostic performance (AUC 0.67, $p = 0.007$), (sensitivity – 92% and specificity - 29% at a 1D-vFFR of 0.7).

Mean Age, years	64(9)
Male, n	62
BMI, kg/m2	28.3(4)
Coronary arteries	N
RCA	19
PDA	1
LMS	1
LAD	67
LCx	11
D1	1
OM1	2
QCA Mean coronary stenosis area,%	54 (16)
QCA Mean lesion length, mm	13 (7)

Table 5.1. Baseline characteristics of all patients (n=85)

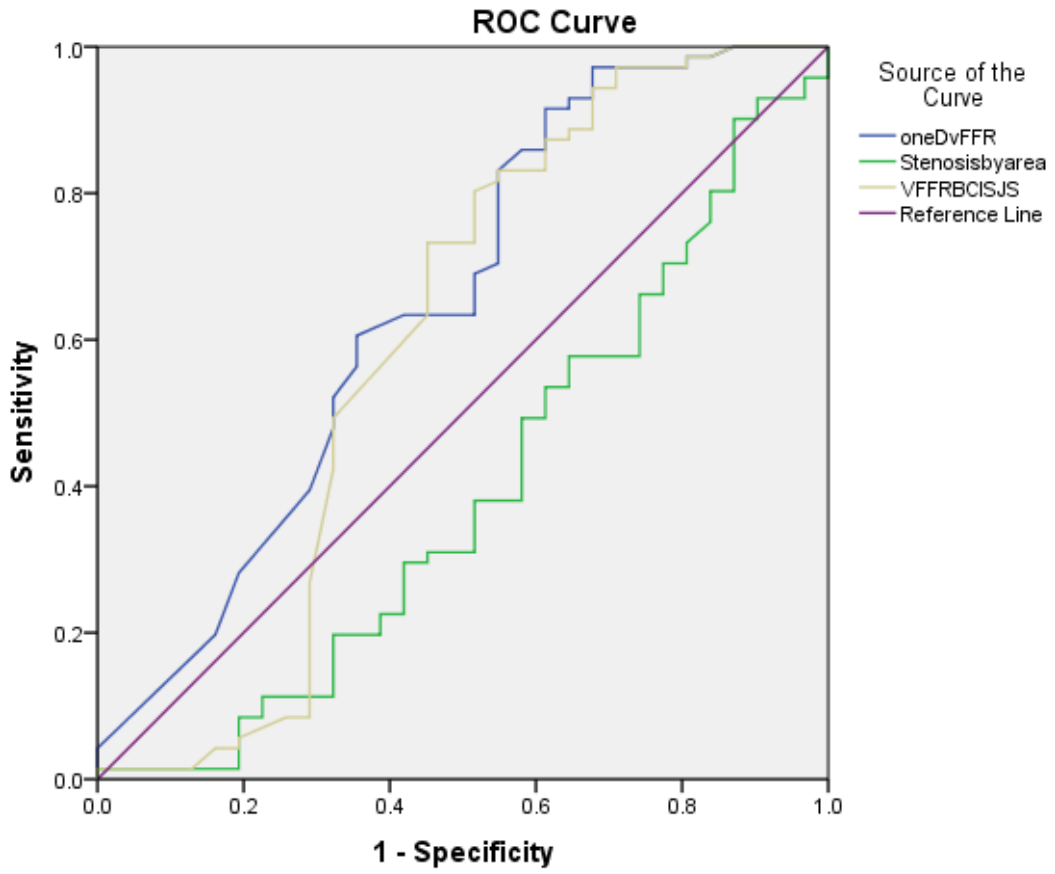

Figure 5.2: Receiver operator characteristic curve of vFFR combined with JS scores (VFFRBCISJS), 1D-vFFR (oneDvFFR) and %stenosis by area derived from QCA (Stenosisbyarea)

Discussion

This is the first study to use one-dimensional computational model coupled with patient specific anatomical data including myocardial jeopardy score to calculate a value of vFFR. The study confirmed the primary hypothesis with superior specificity and sensitivity of vFFR compared with standard anatomical assessment by 2D-QCA with FFR as a reference standard, and a value of vFFR was obtained within minutes. Also, in this study, a minimalistic modelling approach that did not require any image

segmentation was used. This is very attractive from a clinician point of view whereby only some simple measurements are needed that can then be fed into the model.

Myocardial jeopardy scores

Myocardial jeopardy scores were developed several years ago to predict the outcome of acute coronary syndromes on the basis of coronary angiography (127, 132-134). More recently they were demonstrated to correlate well with the area at risk and with the infarct size measured by cardiac magnetic resonance. We found that, in particular for angiographically intermediate stenoses, the larger the amount of jeopardized myocardium, the lower the FFR and the higher the rate of an abnormal FFR. For example, an FFR value ≤0.80 is significantly more likely in a 50% stenosis on the proximal LAD than on the second marginal branch. Thus, considering that the greater the extent of myocardium at risk the worse the prognosis, our data could help explain the important prognostic value of FFR in guiding percutaneous coronary intervention (13, 15). However, in this study, addition of the BCIS scores did not improve performance of the vFFR and may be due to the fact that jeopardy scores are themselves derived from the %stenosis area which themselves account for the physiological severity of stenosis.

Limitations

A number of limitations should be acknowledged. These results represent a retrospective, small single centre experience including 102 intermediate coronary stenoses only and, hence, need confirmation with larger, well-powered multi -centre and prospective studies. QCA was used to evaluate the main angiographic features

of the intermediate stenosis, such as the %DS and the MLD; the latter was finally used to calculate the virtual FFR. Moreover, patients were not referred for an additional myocardial perfusion imaging test before the procedure; this would have been useful to better evaluate the extent of myocardium subtended by the target stenosis. However, FFR has already been shown to correlate well with both non-invasive tests for detecting myocardial ischemia and, more importantly, with the extent of myocardium subtended by the coronary artery stenosis (135, 136). The population studied consisted of patients awaiting elective coronary angiography, hence the potential for selection bias. Patients who had previously undergone revascularization via coronary artery bypass grafting (CABG) surgery were excluded from the study; for that reason, the accuracy of vFFR in these populations remains unknown.

Conclusion

Addition of BCIS Jeopardy scores improves determination of the functional significance of coronary lesions compared with conventional angiography but does not improve virtual FFR derived solely by 1D segmentation free software. Future work in this context may involve investigating how much does segmentation-based modelling improve results over the minimalistic approach.

CHAPTER 6- SUMMARY AND FUTURE WORK

Summary

This work was carried out with the main aim of validating a new physiological index called 1D-vFFR

In particular, two areas of comparison between 1D-vFFR and FFR have been assessed:

1) Investigating the relationship between the assessment of stenosis severity using 1D-vFFR measurement with a virtual subject with increasing lesion length stenosis and increasing area of stenosis

2) To validate the 1D-vFFR results against already obtained FFR results in patients undergoing routine invasive coronary angiography

Chapter 2- showed that increasing lesion length of stenosis only showed a weak inverse relationship with FFR but increasing area of stenosis showed an exponential decrease of FFR

Chapter 3- showed similar results but using varying coronary arteries dimensions.

Chapter 4 – showed that 1D-vFFR has a sensitivity of 83% at a cutoff of 1D-vFFR of 0.75 and an AUC of 60%

Chapter 5- showed that addition of BCIS-Jeopardy score neither improves sensitivity and AUC

Areas of Future Research

The studies presented in this thesis raise some interesting questions, but firstly the results need to be confirmed with larger scale studies. As mentioned already, the incorporation of the functional jeopardy score in routine clinical practice is unlikely because it did not improve the 1D-vFFR but also it would increase the procedure time thus may be a disadvantage. The 1D-vFFR have not been tested on patients who already have underwent previous angioplasty with stenting or CABG, hence it will need to be confirmed in these cohorts. More research must be focussed on more accurate assessment of flow rate, measurement of microvascular resistance as well as assessment of lesion eccentricity.

CHAPTER 7- CONCLUSION

In conclusion, the work in this thesis contributes to a review of existing methods of assessing myocardial ischemia with a focus on virtual FFR and validating a method of ischaemia assessment using 1D-vFFR.

1D-vFFR can be used to estimate ischaemic burden reliably with a sensitivity of 83% with a cut off 1D-vFFR of 0.75.

Addition of a BCIS- Jeopardy score to the calculation of 1D-vFFR does not improve the result of the physiological assessment using 1D-vFFR

Improving the measurement of flow rate, lesion eccentricity and accounting for microvascular resistance will improve the results of 1D-vFFR

LIST OF REFERENCES

1. Laslett LJ, Alagona Jr. P, Clark III BA, Drozda Jr JP, Saldivar F, Wilson SR, Poe C, Hart M. The worldwide environment of cardiovascular disease: prevalence, diagnosis, therapy, and policy issues: a report from the American College of Cardiology J Am Coll Cardiol, 60 (2012), pp. S1–S49

2. Beller GA, Zaret BL. Contributions of nuclear cardiology to diagnosis and prognosis of patients with coronary artery disease. Circulation, 101 (2000), pp. 1465–1478

3. Marie PY, Danchin N, Durand JF, et al. Long-term prediction of major ischemic events by exercise thallium-201 single-photon emission computed tomography: Incremental prognostic value compared with clinical, exercise testing, catheterization and radionuclide angiographic data. J Am Coll Cardiol, 26 (1995), pp. 879–886

4. White CW, Wright CB, Doty DB, et al. Does visual interpretation of the coronary arteriogram predict the physiologic importance of a coronary stenosis? N Engl J Med 1984;310:819-24.

5. Johnson NP, Kirkeeide RL, Gould KL. Coronary Anatomy to Predict Physiology Fundamental Limits. Circulation-Cardiovascular Imaging 2013;6:817-32.

6. Bach RG. Angiographically insignificant yet ischemia-causing coronary lesions: a case for routine use of invasive physiologic testing during diagnostic cardiac catheterization. *J Thorac Dis*. 2018;10(Suppl 26):S3088-S3091. doi:10.21037/jtd.2018.08.07

7. Pijls NH, De Bruyne B, Peels K, et al. Measurement of fractional flow reserve to assess the functional severity of coronary-artery stenoses. N Engl J Med 1996;334:1703-8.

8. Pijls NH, Van Gelder B, Van der Voort P, et al. Fractional flow reserve. A useful index to evaluate the influence of an epicardial coronary stenosis on myocardial blood flow. Circulation 1995;92:3183-93.

9. Kern MJ, Samady H. Current concepts of integrated coronary physiology in the catheterization laboratory. J Am Coll Cardiol. 2010 Jan 19;55(3):173-85. doi: 10.1016/j.jacc.2009.06.062. Review.

10. Pijls NHJ, Sels JWEM. Functional Measurement of Coronary Stenosis. JAC. Elsevier Inc.; 2012 Mar. 20;59(12):1045–1057.

11. De Bruyne B, Bartunek J, Sys SU, Pijls NH, Heyndrickx GR, Wijns W. Simultaneous coronary pressure and flow velocity measurements in humans. Feasibility, reproducibility, and hemodynamic dependence of coronary flow velocity reserve, hyperaemic flow versus pressure slope index, and fractional flow reserve. Circulation. 1996 Oct. 15;94(8):1842–1849.

12. Bech GJ, De Bruyne B, Pijls NH, de Muinck ED, Hoorntje JC, Escaned J, et al. Fractional flow reserve to determine the appropriateness of angioplasty in moderate coronary stenosis: a randomized trial. Circulation. 2001 Jun. 19;103(24):2928–2934.

13. Pijls NH, Fearon WF, Tonino PA et al. (2010) Fractional flow reserve versus angiography for guiding percutaneous coronary intervention in patients with multivessel coronary artery disease: 2-year follow-up of the FAME (Fractional Flow Reserve Versus Angiography for Multivessel Evaluation) study. Journal of the American College of Cardiology 56: 177–184.

14. Pijls NH, van Schaardenburgh P, Manoharan G et al. (2007) Percutaneous coronary intervention of functionally nonsignificant stenosis: 5-year follow-up of the DEFER Study. Journal of the American College of Cardiology 49: 2105–2111.

15. Tonino PA, De Bruyne B, Pijls NH, Siebert U, Ikeno F, van' t Veer M, Klauss V, Manoharan G, Engstrøm T, Oldroyd KG, Ver Lee PN, MacCarthy PA, Fearon WF; FAME Study Investigators. Fractional flow reserve versus angiography for guiding percutaneous coronary intervention. N Engl J Med. 2009 Jan 15;360(3):213-24. doi: 10.1056/NEJMoa0807611.

16. De Bruyne B, Fearon WF, Pijls NH, Barbato E, Tonino P, Piroth Z, Jagic N, Mobius-Winckler S, Rioufol G, Witt N, Kala P, MacCarthy P, Engström T, Oldroyd K, Mavromatis K, Manoharan G, Verlee P, Frobert O, Curzen N, Johnson JB, Limacher A, Nüesch E, Jüni P; FAME 2 Trial Investigators. Fractional flow reserve-guided PCI for stable coronary artery disease. N Engl J Med. 2014 Sep 25;371(13):1208-17. doi: 10.1056/NEJMoa1408758. Epub 2014 Sep 1. Erratum in: N Engl J Med. 2014 Oct 9;371(15):1465.

17. Tonino PAL, De Bruyne B, Pijls NH et al. Fractional flow reserve versus angiography for guiding percutaneous coronary intervention. N Engl J Med. 2009;360:213–24.

18. De Bruyne B, Pijls NH, Kalesan B et al. Fractional flow reserve-guided PCI versus medical therapy in stable coronary disease. N Engl J Med. 2012;367:991–1001.

19. Tonino PA, Fearon WF, De Bruyne B, FAME Study Investigators, *et al.* Angiographic severity versus functional severity of coronary artery stenoses in the FAME study. J Am Coll Cardiol, 55 (2010), pp. 2816–2821

20. Fukuoka S, Kurita T, Takasaki A, et al. Clinical usefulness of instantaneous wave-free ratio for the evaluation of coronary artery lesion with prior myocardial infarction: A multi-center study. *Int J Cardiol Heart Vasc*. 2019;26:100431. Published 2019 Dec 19. doi:10.1016/j.ijcha.2019.100431)

21. Coughlan JJ, MacDonnell C, Arnous S, Kiernan TJ. Fractional flow reserve in 2017: current data and everyday practice. Expert Rev Cardiovasc Ther. 2017 Jun;15(6):457-472.

22. Hwang D, Jeon KH, Lee JM, Park J, Kim CH, Tong Y, Zhang J, Bang JI, Suh M, Paeng JC, Na SH, Cheon GJ, Cook CM, Davies JE, Koo BK. Diagnostic Performance of Resting and Hyperemic Invasive Physiological Indices to Define Myocardial Ischemia: Validation With ^{13}N-Ammonia Positron Emission Tomography. JACC Cardiovasc Interv. 2017 Apr 24;10(8):751-760.

23. Götberg M, Christiansen EH, Gudmundsdottir IJ, Sandhall L, Danielewicz M, Jakobsen L, Olsson SE, Öhagen P, Olsson H, Omerovic E, Calais F, Lindroos P, Maeng M, Tödt T, Venetsanos D, James SK, Kåregren A, Nilsson M, Carlsson J, Hauer D, Jensen J, Karlsson AC, Panayi G, Erlinge D, Fröbert O., iFR-SWEDEHEART Investigators. Instantaneous Wave-free Ratio versus Fractional Flow Reserve to Guide PCI. N Engl J Med. 2017 May 11;376(19):1813-1823.

24. Boden WE, O'Rourke RA, Teo KK, et al; COURAGE Trial Research Group. Optimal medical therapy with or without PCI for stable coronary disease. N Engl J Med 2007;356:1503–16

25. Detre J, Wright E, Murphy ML, Takaro T. Observer agreement in evaluating coronary angiograms. Circulation, 52 (1975), pp. 979–988

26. Zir LM, Miller SW, Dinsmore RE, Gilbert JP, Harthorne JW. Interobserver variability in coronary angiography. Circulation, 53 (1976), pp. 627–632

27. Green NE, Chen SY, Messenger JC, Groves BM, Carroll JD. Three-dimensional vascular angiography. Curr Probl Cardiol, 29 (2004), pp. 104–142

28. Curzen N, Rana O, Nicholas Z, Golledge P, Zaman A, Oldroyd K, Hanratty C, Banning A, Wheatcroft S, Hobson A, Chitkara K, Hildick-Smith D, McKenzie D, Calver A, Dimitrov BD, Corbett S. Does routine pressure wire assessment influence management strategy at coronary angiography for diagnosis of chest pain?: the RIPCORD study. Circ Cardiovasc Interv. 2014 Apr;7(2):248-55.

29. Pijls NH, Sels JW. Functional measurement of coronary stenosis. J Am Coll Cardiol 2012;59:1045-57

30. Tonino PA, De Bruyne B, Pijls NH, et al. Fractional flow reserve versus angiography for guiding percutaneous coronary intervention. N Engl J Med 2009;360:213-24

31. Pijls NHJ, Sels JW. Functional measurement of coronary stenosis. J Am Coll Cardiol 2012; 59: 1045 – 1057.

32. Pijls NHJ, Tanaka N, Fearon WF. Functional assessment of coronary stenosis: Can we live without it? Eur Heart J 2012 December 19.

33. Pijls NH, Van Gelder B, Van der Voort P, Peels K, Bracke FA, Bonnier HJ, et al. Fractional flow reserve: A useful index to evaluate the influence of an epicardial coronary stenosis on myocardial blood flow. Circulation 1995; 92: 3183 – 3193.

34. De Bruyne B, Hersbach F, Pijls NHJ, Bartunek J, Bech JW, Heyndrickx GR, et al. Abnormal epicardial coronary resistance in patients with diffuse atherosclerosis but “normal” coronary angiography, Circulation 2001; 104: 2401 – 2406.

35. De Bruyne B, Bartunek J, Sys SU, Pijls NHJ, Heyndrickx GR, Wijns W. Simultaneous coronary pressure and flow velocity measurements in humans: Feasibility, reproducibility, and hemodynamic dependence of coronary flow velocity reserve, hyperemic flow versus pressure slope index, and fractional flow reserve. Circulation 1996; 94: 1842 – 1849.

36. Berry C, van't Veer M, Witt N, Kala P, Bocek O, Pyxaras SA, et al. VERIFY (VERification of Instantaneous Wave-Free Ratio and Fractional Flow Reserve for the Assessment of Coronary Artery Stenosis Severity in EverydaY Practice): A multicenter study in consecutive patients. J Am Coll Cardiol 2013 February 1 [Epub ahead of print].

37. Fearon WF, Bornschein B, Tonino PA, Gothe RM, Bruyne BD, Pijls NH, et al. Economic evaluation of fractional flow reserve guided percutaneous coronary intervention patients with multivessel disease. Circulation 2010; 122: 2545 – 2550.

38.Topol EJ, Ellis SG, Cosgrove DM, Bates ER, Muller DW, Schork NJ, et al. Analysis of coronary angioplasty practice in the United States with an insurance-claims data base. Circulation 1993;87:1489-97

39. Task Force Members, Montalescot G, Sechtem U, et al. 2013 ESC guidelines on the management of stable coronary artery disease: The Task Force on the management of stable coronary artery disease of the European Society of Cardiology. Eur Heart J 2013.

40. Patel MR. (2013) Fractional Flow Reserve and the Appropriate Use Criteria: determining best practices in coronary revascularization. Cardiac Interventions Today Jan–Feb 2013: 64–74

41. Lawton J, Tamis-Holland J, et al. 2021 ACC/AHA/SCAI Guideline for Coronary Artery Revascularization. *J Am Coll Cardiol.* 2022 Jan, 79 (2) e21–e129.

42. Ludman PF. BCIS Audit Returns Adult Interventional Procedures:

1st April 2018 to 31st March 2019 http://www.bcis.org.uk/wp-content/uploads/2020/12/BCIS-Audit-2018-19-data-ALL-4-5-2020-for-web.pdf. British Cardiovascular Interventional Society, London (2019) Available at: Accessed January 20, 2021.

43. Dehmer GJ, Weaver D, Roe MT, et al. A contemporary view of diagnostic cardiac catheterization and percutaneous coronary intervention in the United States: a report from the CathPCI Registry of the National Cardiovascular Data Registry, 2010 through June 2011. J Am Coll Cardiol, 60 (2012), pp. 2017–2031

44. Orvin K, Bental T, Eisen A, Vaknin-Assa H, Assali A, Lev EI. et al. Fractional flow reserve application in everyday practice: adherence to clinical recommendations. Cardiovasc Diagn Ther. 2013;3(3):137–45.

45. Hannawi B, WW, Wang S, Younis GA. Current Use of Fractional Flow Reserve: A Nationwide Survey. Tex Heart Inst J. 2014 Dec 1;41(6):579-84.

46. Morris PD, Ryan D, Morton AC, et al. Virtual fractional flow reserve from coronary angiography: modeling the significance of coronary lesions: results from the VIRTU-1 (VIRTUal Fractional Flow Reserve From Coronary Angiography) study. JACC Cardiovasc Interv 2013;6:149–57.

47. Papafaklis MI, Muramatsu T, Ishibashi Y, et al. Virtual resting Pd/Pa from coronary angiography and blood flow modelling: diagnostic performance against fractional flow reserve. Heart Lung Circ 2018;27:377–80.

48. Tu S, Barbato E, Köszegi Z, et al. Fractional flow reserve calculation from 3-

dimensional quantitative coronary angiography and TIMI frame count: A fast computer model to quantify the functional significance of moderately obstructed coronary arteries. JACC Cardiovasc Interv 2014;7:768–77.

49. Tu S, Westra J, Yang J, et al. Diagnostic accuracy of fast computational approaches to derive fractional flow reserve from diagnostic coronary angiography: the international multicenter FAVOR pilot study. JACC Cardiovasc Interv 2016;9:2024–35.

50. Pellicano M, Lavi I, De Bruyne B, et al. Validation study of image-based fractional flow reserve during coronary angiography. Circ Cardiovasc Interv 2017;10:e005259.

51. Kornowski R, Vaknin-Assa H, Assali A, et al. Online angiography image-based FFR assessment during coronary catheterization: a single-center study. J Invasive Cardiol 2018;30:224–9.

52. Fearon WF, Achenbach S, Engstrom T, et al. Accuracy of fractional flow reserve derived from coronary angiography. Circulation 2019;139:477–84.

53. Hulten E, Pickett C, Bittencourt MS, Villines TC, Petrillo S, Di Carli MF, Blankstein R. Outcomes after coronary computed tomography angiography in the emergency department: a systematic review and meta-analysis of randomized, controlled trials. *J Am Coll Cardiol* 2013; 61:880–892.

54. Schuijf JD, Bax JJ. CT angiography: an alternative to nuclear perfusion imaging? Heart. 2008;94:255–257.

55. Juhani Knuuti, William Wijns, Antti Saraste, Davide Capodanno, Emanuele Barbato, Christian Funck-Brentano, Eva Prescott, Robert F Storey, Christi Deaton, Thomas Cuisset, Stefan Agewall, Kenneth Dickstein, Thor Edvardsen, Javier

Escaned, Bernard J Gersh, Pavel Svitil, Martine Gilard, David Hasdai, Robert Hatala, Felix Mahfoud, Josep Masip, Claudio Muneretto, Marco Valgimigli, Stephan Achenbach, Jeroen J Bax, ESC Scientific Document Group, 2019 ESC Guidelines for the diagnosis and management of chronic coronary syndromes: The Task Force for the diagnosis and management of chronic coronary syndromes of the European Society of Cardiology (ESC), *European Heart Journal*, Volume 41, Issue 3, 14 January 2020, Pages 407–477,

56. Zhang JM, Zhong L, Su B, Wan M, Yap JS, Tham JP, Chua LP, Ghista DN, Tan RS. Perspective on CFD studies of coronary artery disease lesions and hemodynamics: a review. Int J Numer Method Biomed Eng. 2014 Jun;30(6):659-80. doi: 10.1002/cnm.2625. Epub 2014 Jan 23. Review

57. Koo BK, Erglis A, Doh JH, et al. Diagnosis of ischemia-causing coronary stenoses by noninvasive fractional flow reserve computed from coronary computed tomographic angiograms. Results from the prospective multicenter DISCOVER-FLOW (Diagnosis of Ischemia-Causing Stenoses Obtained Via Noninvasive Fractional Flow Reserve) study. J Am Coll Cardiol, 58 (2011), pp. 1989–1997.

58. Min K, Leipsic J, Pencina MJ, et al. Diagnostic accuracy of fractional flow reserve from anatomic CT angiography. JAMA, 308 (2012), pp. 1237–1245

59. Nieman K, Serruys PW, Onuma Y, van Geuns RJ, Garcia-Garcia HM, de Bruyne B, Thuesen L, Smits PC, Koolen JJ, McClean D, Chevalier B, Meredith I, Ormiston J. Multislice computed tomography angiography for noninvasive assessment of the 18-month performance of a novel radiolucent bioresorbable vascular scaffolding device: the ABSORB trial (a clinical evaluation of the bioabsorbable everolimus eluting

coronary stent system in the treatment of patients with de novo native coronary artery lesions). J Am Coll Cardiol. 2013 Nov 5;62(19):1813-4. doi: 10.1016/j.jacc.2013.07.030. Epub 2013 Aug 7.

60. Douglas PS, Pontone G, Hlatky MA, Patel MR, Norgaard BL, Byrne RA, Curzen N, Purcell I, Gutberlet M, Rioufol G, Hink U, Schuchlenz HW, Feuchtner G, Gilard M, Andreini D, Jensen JM, Hadamitzky M, Chiswell K, Cyr D, Wilk A, Wang F, Rogers C, De Bruyne B; PLATFORM Investigators. Clinical outcomes of fractional flow reserve by computed tomographic angiography-guided diagnostic strategies vs. usual care in patients with suspected coronary artery disease: the prospective longitudinal trial of FFR(CT): outcome and resource impacts study. *Eur Heart J* 2015; 36: 3359–3367.

61.Papafaklis MI, Muramatsu T, Ishibashi Y, Lakkas LS, Nakatani S, Bourantas CV, Ligthart J, Onuma Y, Echavarria-Pinto M, Tsirka G, Kotsia A, Nikas DN, Mogabgab O, van Geuns RJ, Naka KK, Fotiadis DI, Brilakis ES, Garcia-Garcia HM, Escaned J, Zijlstra F, Michalis LK, Serruys PW. Fast virtual functional assessment of intermediate coronary lesions using routine angiographic data and blood flow simulation in humans: comparison with pressure wire - fractional flow reserve. EuroIntervention. 2014 Sep;10(5):574-83.

62. Uren NG, Melin JA, De Bruyne B, Wijns W, Baudhuin T, Camici PG. Relation between myocardial blood flow and the severity of coronary-artery stenosis. N Engl J Med. 1994;330:1782-8.

63. Petraco R, van de Hoef TP, Nijjer S, Sen S, van Lavieren MA, Foale RA, Meuwissen M, Broyd C, Echavarria-Pinto M, Foin N, Malik IS, Mikhail GW, Hughes AD, Francis DP, Mayet J, Di Mario C, Escaned J, Piek JJ, Davies JE. Baseline Instantaneous Wave-Free Ratio as a Pressure-Only Estimation of Underlying Coronary Flow Reserve: Results of the JUSTIFY-CFR Study (Joined Coronary Pressure and Flow Analysis to Determine Diagnostic Characteristics of Basal and Hyperemic Indices of Functional Lesion Severity-Coronary Flow Reserve). Circ Cardiovasc Interv. 2014 Jul 1. pii: CIRCINTERVENTIONS. 113.000926. [Epub ahead of print].

64. Echavarria-Pinto M, Escaned J, Macías E, Medina M, Gonzalo N, Petraco R, Sen S, Jimenez-Quevedo P, Hernandez R, Mila R, Ibañez B, Nuñez-Gil IJ, Fernández C, Alfonso F, Bañuelos C, García E, Davies J, Fernández-Ortiz A, Macaya C. Disturbed coronary hemodynamics in vessels with intermediate stenoses evaluated with fractional flow reserve: a combined analysis of epicardial and microcirculatory involvement in ischemic heart disease. Circulation. 2013;128:2557-66.

65. Kousera CA, Nijjer S, Torii R, Petraco R, Sen S, Foin N, Hughes AD, Francis DP, Xu XY, Davies JE. Patient-specific coronary stenoses can be modeled using a combination of OCT and flow velocities to accurately predict hyperemic pressure gradients. IEEE Trans Biomed Eng. 2014;61:1902-13.

66. Bezerra HG, Costa MA, Guagliumi G, Rollins AM, Simon DI. Intracoronary optical coherence tomography: a comprehensive review clinical and research applications. JACC Cardiovasc Interv. 2009 Nov;2(11):1035-46.

67. Guagliumi G, Sirbu V, Petroff C, Capodanno D, Musumeci G, Yamamoto H, Elbasiony A, Brushett C, Matiashvili A, Lortkipanidze N, Valsecchi O, Bezerra HG, Schmitt JM. Volumetric assessment of lesion severity with optical coherence tomography: relationship with fractional flow. EuroIntervention. 2013 Feb 22;8(10):1172-81.

68. Stefano GT, Bezerra HG, Attizzani G, Chamié D, Mehanna E, Yamamoto H, Costa MA. Utilization of frequency domain optical coherence tomography and fractional flow reserve to assess intermediate coronary artery stenoses: conciliating anatomic and physiologic information. Int J Cardiovasc Imaging. 2011 Feb;27(2):299-308. doi: 10.1007/s10554-011-9847-9. Epub 2011 Mar 17.

69. Gonzalo N, Escaned J, Alfonso F, Nolte C, Rodriguez V, Jimenez-Quevedo P, Bañuelos C, Fernández-Ortiz A, Garcia E, Hernandez-Antolin R, Macaya C. Morphometric assessment of coronary stenosis relevance with optical coherence tomography: a comparison with fractional flow reserve and intravascular ultrasound. J Am Coll Cardiol. 2012 Mar 20;59(12):1080-9.

70. Zafar H, Sharif F, Leahy MJ. Feasibility of intracoronary frequency domain optical coherence tomography derived fractional flow reserve for the assessment of coronary artery stenosis. Int Heart J. 2014;55(4):307-11. Epub 2014 Jun 6.

71. Masdjedi K, van Zandvoort LJC, Balbi MM, Gijsen FJH, Ligthart JMR, Rutten MCM, Lemmert ME, Wilschut JM, Diletti R, de Jaegere P, Zijlstra F, Van Mieghem NM, Daemen J. Validation of a three-dimensional quantitative coronary angiography-

based software to calculate fractional flow reserve: the FAST study. EuroIntervention. 2020 Sep 18;16(7):591-599. doi: 10.4244/EIJ-D-19-00466. PMID: 31085504.

72. Lyras KG, Lee J (2021). An improved reduced-order model for pressure drop across arterial stenoses. PLoS ONE 16(10): e0258047.

73. Hashemi J, Patel B, Chatzizisis YS, Kassab GS. Real time reduced order model for angiography fractional flow reserve. Computer Methods and Programs in Biomedicine. 2022 Apr;216:106674.

74. Mynard JP, Nithiarasu P. A 1D arterial blood flow model incorporating ventricular pressure, aortic valve and regional coronary flow using the locally conservative Galerkin (LCG) method, Communications in Numerical Methods in Engineering, 2008, 24, 5, pp.367

75. Mynard JP, Penny DJ and Smolich JJ. Scalability and in vivo validation of a multiscale numerical model of the left coronary circulation. *Am J Physiol Heart Circ Physiol*. 2014;306:H517-H528.

76. Mynard JP and Smolich JJ. Influence of anatomical dominance and hypertension on coronary conduit arterial and microcirculatory flow patterns: a multi-scale modeling study. *Am J Physiol Heart Circ Physiol*. 2016;311:H11-H23.

77. Mynard JP and Smolich JJ. One-Dimensional Haemodynamic Modeling and Wave Dynamics in the Entire Adult Circulation. *Ann Biomed Eng*. 2015;43:1443-1460.

78. Quarteroni A, Formaggia L. Mathematical modelling and numerical simulation of the cardiovascular system. Handb Numer Anal. 2004;12:7–9.

79. Quarteroni A, Manzoni A, Vergara C. The cardiovascular system: mathematical modelling, numerical algorithms and clinical applications. Acta Numer. 2017;26:365–590.

80. Capoccia M, Marconi S, Singh SA, Pisanelli DM, De CL. Simulation as a preoperative planning approach in advanced heart failure patients. a retrospective clinical analysis. Biomed Eng Online. 2018;17(1):52–72.

81. Tang D, Li ZY, Gijsen F, Giddens DP. Cardiovascular diseases and vulnerable plaques: data, modeling, predictions and clinical applications. Biomed Eng Online. 2015;14(1):1–7.

82. Zhou S, Xu L, Hao L, Xiao H, Yao Y, Qi L, Yao Y. A review on low-dimensional physics-based models of systemic arteries: application to estimation of central aortic pressure. Biomed Eng Online. 2019 Apr 2;18(1):41. doi: 10.1186/s12938-019-0660-3.

83. Ghigo AR, Fullana JM, Lagree PY, Ghigo AR, Fullana JM, Lagree PY, Ghigo AR, Fullana JM, Lagree PY. A 2D nonlinear multiring model for blood flow in large elastic arteries. J Comput Phys. 2016;350:136–65.

84. Boujena S, Kafi O, El Khatib N. A 2D mathematical model of blood flow and its interactions in an atherosclerotic artery. Math Model Nat Phenom. 2014;09(6):46–68.

85. Lopez perez A, Sebastian R, Ferrero JM. Three-dimensional cardiac computational modelling: methods, features and applications. Biomed Eng Online. 2015;14(1):35–65.

86. Xie X, Zheng M, Wen D, Li Y, Xie S. A new CFD based non-invasive method for functional diagnosis of coronary stenosis. Biomed Eng Online. 2018;17(1):36–48.

87. Frank O. Grundform des arteriellen pulses. Z Biol. 1899;37:483–526.

88. Shi Y, Lawford P, Hose R. Review of zero-D and 1-D models of blood flow in the cardiovascular system. Biomed Eng Online. 2011;10(1):33–70.

89. Malatos S, Raptis A, Xenos M. Advances in low-dimensional mathematical modeling of the human cardiovascular system. J Hypertens Manag. 2016;2(2):1–10.

90. Westerhof N, Bosman F, De Vries CJ, Noordergraaf A. Analog studies of the human systemic arterial tree. J Biomech. 1969;2(2):121–43.

91. Hughes TJR, Lubliner J. On the one-dimensional theory of blood flow in the larger vessels. Math Biosci.1973;18(1):161–70.

92. Olufsen MS, Peskin CS, Kim WY, Pedersen EM, Nadim A, Larsen J. Numerical simulation and experimental validation of blood flow in arteries with structured-tree outflow conditions. Ann Biomed Eng. 2000;28(11):1281–99.

93. Mynard, JP, Penny, DJ, Smolich, JJ. Scalability and in vivo validation of a multiscale numerical model of the left coronary circulation. Am J Physiol Heart CircPhysiol 2014; 306: H517–H528.

94. Mynard, JP, Nithiarasu, P. A 1D arterial blood flow model incorporating ventricular pressure, aortic valve and regional coronary flow using the locally conservative Galerkin (LCG) method. Commun Numer Meth Engng 2008; 24: 367–417.

95. Young, DF, Tsai, FY. Flow characteristics in models of arterial stenosis: II. Unsteady flow. J Biomech 1973; 6: 547–559.

96. Brosh D, Higano ST, Lennon RJ, Holmes DR Jr, Lerman A. Effect of lesion length on fractional flow reserve in intermediate coronary lesions. Am Heart J. 2005 Aug;150(2):338-43.

97. Alghamdi A, Mohammed Balgaith M, Abdulaziz Alkhaldi A. Influence of the length of coronary artery lesions on fractional flow reserve across intermediate coronary obstruction, *European Heart Journal Supplements*, Volume 16, Issue suppl_B, November 2014, Pages B76–B79,

98. Takagi A, Tsurumi Y, Ishii Y, Suzuki K, Kawana M, Kasanuki H. Clinical potential of intravascular ultrasound for physiological assessment of coronary stenosis: relationship between quantitative ultrasound tomography and pressure-derived fractional flow reserve. Circulation. 1999 Jul 20;100(3):250-5.

99. Carlsson, M, Andersson, R, Bloch, KM, et al. Cardiac output and cardiac index measured with cardiovascular magnetic resonance in healthy subjects, elite athletes and patients with congestive heart failure. J Cardiovasc Magn Reson 2012; 14: 51.

100. Kern, MJ, Bach, RG, Mechem, CJ, et al. Variations in normal coronary vasodilatory reserve stratified by artery, gender, heart transplantation and coronary artery disease. J Am Coll Cardiol 1996; 28: 1154–1160.

101. Wilson, R, Wyche, K, Christensen, B, et al. Effects of adenosine on human coronary arterial circulation. Circulation 1990; 82: 1595–1606.

102. Mynard, JP, Smolich, JJ. Influence of anatomical dominance and hypertension on coronary conduit arterial and microcirculatory flow patterns: a multi-scale modeling study. Am J Physiol Heart CircPhysiol 2016; 311: H11–H23.

103. Gould KL, Johnson NP, Bateman TM, Bengel FM, Bober R, Camici PG, et al. Anatomic versus physiologic assessment of coronary artery disease. Role of coronary flow reserve, fractional flow reserve, and positron emission tomography imaging in revascularization decision-making. J Am Coll Cardiol 2013;62:1639–53. pmid:23954338

104. van de Hoef TP, van Lavieren MA, Damman P, Delewi R, Piek MA, Chamuleau SA, et al. Physiological basis and long-term clinical outcome of discordance between fractional flow reserve and coronary flow velocity reserve in coronary stenoses of intermediate severity. Circ Cardiovasc Interv 2014;7:301–11. pmid:24782198

105. Morris PD, van de Vosse FN, Lawford PV, Hose DR, Gunn JP. "Virtual" (Computed) Fractional Flow Reserve: Current Challenges and Limitations. JACC CardiovascInterv. 2015;8(8):1009–1017. doi:10.1016/j.jcin.2015.04.006

106. Tilsted HH, Ahlehoff O, Terkelsen CJ, Pedersen F, Özcan C, Jørgensen TH, Nielsen-Kudsk JE, Ravkilde J, Nissen H, Pedersen SA, Havndrup O, Lassen JF. Denmark: coronary and structural heart interventions from 2010 to 2015. EuroIntervention. 2017;13:Z17–Z20. =6

107. Desmet W, Aminian A, Kefer J, Dens J, Bosmans J, Claeys M, Dubois C, Gach O, Janssens L, Schroeder E, Vermeersch P, Carlier M, Benit E, Hanet C.. Belgium: coronary and structural heart interventions from 2010 to 2015. EuroIntervention. 2017;13:Z14–Z16. =7

108. Papafaklis MI, Muramatsu T, Ishibashi Y, Lakkas LS, Nakatani S, Bourantas CV, Ligthart J, Onuma Y, Echavarria-Pinto M, Tsirka G, Kotsia A, Nikas DN, Mogabgab O, van Geuns RJ, Naka KK, Fotiadis DI, Brilakis ES, Garcia-Garcia HM, Escaned J, Zijlstra F, Michalis LK, Serruys PW. Fast virtual functional assessment of intermediate coronary lesions using routine angiographic data and blood flow simulation in humans: comparison with pressure wire - fractional flow reserve. EuroIntervention. 2014 Sep;10(5):574-83.

109. Mosteller RD. Simplified Calculation of Body Surface Area. N Engl J Med 1987 Oct 22;317(17):1098 (letter)

110. Choy JS, Kassab GS. Scaling of myocardial mass to flow and morphometry of coronary arteries. J ApplPhysiol (1985). 2008 May;104(5):1281-6

111. Chareonthaitawee P, Kaufmann PA, Rimoldi O, Camici PG. Heterogeneity of resting and hyperemic myocardial blood flow in healthy humans. Cardiovasc Res.2001 Apr;50(1):151-61.

112. Cain P, Ahl R, HedstromE, UganderM, Allansdotter-Johnsson A, Friberg P, Arheden H. Age and gender specific normal values of left ventricular mass, volume and function for gradient echo magnetic resonance imaging: a cross sectional study. BMC Med Imaging. 2009;9(2).

113. Kim H, Vignon-Clementel I, Coogan J, Figueroa C, Jansen K, Taylor C. Patient-specific modeling of blood flow and pressure in human coronary arteries. Ann Biomed Eng. 2010;38:3195-3209.

114. Le HQ, Wong JT, Molloi S. Allometric scaling in the coronary arterial system. Int J Cardiovasc Imaging. 2008 Oct;24(7):771-81.

115. Tonino PA, De Bruyne B, Pijls NH, Siebert U, Ikeno F, van' t Veer M, Klauss V, Manoharan G, Engstrøm T, Oldroyd KG, Ver Lee PN, MacCarthy PA, Fearon WF; FAME Study Investigators. Fractional flow reserve versus angiography for guiding percutaneous coronary intervention.N Engl J Med. 2009 Jan 15;360(3):213-24.

116. Nørgaard BL, Leipsic J, Gaur S, Seneviratne S, Ko BS, Ito H, Jensen JM, Mauri L, De Bruyne B, Bezerra H, Osawa K, Marwan M, Naber C, Erglis A, Park SJ, Christiansen EH, Kaltoft A, Lassen JF, Bøtker HE, Achenbach S; NXT Trial Study Group. Diagnostic performance of noninvasive fractional flow reserve derived from coronary computed tomography angiography in suspected coronary artery disease: the NXT trial (Analysis of Coronary Blood Flow Using CT Angiography: Next Steps).J Am CollCardiol. 2014 Apr 1;63(12):1145-1155.

117. Douglas PS, De Bruyne B, Pontone G, Patel MR, Norgaard BL, Byrne RA, Curzen N, Purcell I, Gutberlet M, Rioufol G, Hink U, Schuchlenz HW, Feuchtner G, Gilard M, Andreini D, Jensen JM, Hadamitzky M, Chiswell K, Cyr D, Wilk A, Wang F, Rogers C, Hlatky MA; PLATFORM Investigators. 1-Year Outcomes of FFRCT-Guided Care in Patients With Suspected Coronary Disease: The PLATFORM Study.J Am CollCardiol. 2016 Aug 2;68(5):435-445.

118. Lu MT, Ferencik M, Roberts RS, Lee KL, Ivanov A, Adami E, Mark DB, Jaffer FA, Leipsic JA, Douglas PS, Hoffmann U. Noninvasive FFR Derived From Coronary CT Angiography: Management and Outcomes in the PROMISE Trial.JACC Cardiovasc Imaging. 2017 Nov;10(11):1350-1358.

119. Morris PD, Silva Soto DA, Feher JFA, Rafiroiu D, Lungu A, Varma S, Lawford PV, Hose DR, Gunn JP. Fast Virtual Fractional Flow Reserve Based Upon Steady-

State Computational Fluid Dynamics Analysis: Results From the VIRTU-Fast Study.JACC Basic Transl Sci. 2017 Aug 28;2(4):434-446.

120. Tu S, Barbato E, Köszegi Z, Yang J, Sun Z, Holm NR, Tar B, Li Y, Rusinaru D, Wijns W, Reiber JH. Fractional flow reserve calculation from 3-dimensional quantitative coronary angiography and TIMI frame count: a fast computer model to quantify the functional significance of moderately obstructed coronary arteries. JACC Cardiovasc Interv. 2014 Jul;7(7):768-77.

121. Xu B, Tu S, Song L, Jin Z, Yu B, Fu G, Zhou Y, Wang J, Chen Y, Pu J, Chen L, Qu X, Yang J, Liu X, Guo L, Shen C, Zhang Y, Zhang Q, Pan H, Fu X, Liu J, Zhao Y, Escaned J, Wang Y, Fearon WF, Dou K, Kirtane AJ, Wu Y, Serruys PW, Yang W, Wijns W, Guan C, Leon MB, Qiao S, Stone GW; FAVOR III China study group. Angiographic quantitative flow ratio-guided coronary intervention (FAVOR III China): a multicentre, randomised, sham-controlled trial. Lancet. 2021 Dec 11;398(10317):2149-2159. doi: 10.1016/S0140-6736(21)02248-0. Epub 2021 Nov 4.

122. Pellicano M, Lavi I, De Bruyne B, Vaknin-Assa H, Assali A, Valtzer O, Lotringer Y, Weisz G, Almagor Y, Xaplanteris P, Kirtane AJ, Codner P, Leon MB, Kornowski R. Validation Study of Image-Based Fractional Flow Reserve During Coronary Angiography. Circ Cardiovasc Interv. 2017 Sep;10(9). pii: e005259.

123. Fearon WF, Achenbach S, Engstrom T, Assali A, Shlofmitz R, Jeremias A, Fournier S, Kirtane AJ, Kornowski R, Greenberg G, Jubeh R, Kolansky DM, McAndrew T, Dressler O, Maehara A, Matsumura M, Leon MB, De Bruyne B; FAST-FFR Study Investigators. Accuracy of Fractional Flow Reserve Derived From Coronary Angiography. Circulation. 2019 Jan 22;139(4):477-484.

124. Mynard JP, Nithiarasu P. A 1D Arterial Blood Flow Model Incorporating Ventricular Pressure, Aortic Valve and Regional Coronary Flow Using Locally Conservative Galerkin (LCG) Method. Swansea University. Published in Communicating in Numerical Methods In Engineering, 2008; 24:367-417

125. Boileau E, Pant S, Roobottom C, Sazonov I, Deng J, Xie X, Nithiarasu P. Estimating the accuracy of a reduced-order model for the calculation of fractional flow reserve (FFR). Int J Numer Method Biomed Eng. 2018 Jan;34(1).

126. Hachamovitch R, Hayes SW, Friedman JD, Cohen I, Berman DS. Comparison of the short-term survival benefit associated with revascularization compared with medical therapy in patients with no prior coronary artery disease undergoing stress myocardial perfusion single photon emission computed tomography. Circulation. 2003 Jun 17;107(23):2900-7.

127. Califf RM, Phillips HR, 3rd, Hindman MC, Mark DB, Lee KL, Behar VS, et al. Prognostic value of a coronary artery jeopardy score. Journal of the American College of Cardiology. 1985 May;5(5):1055-63.

128. Graham MM, Faris PD, Ghali WA, Galbraith PD, Norris CM, Badry JT, Mitchell LB, Curtis MJ, Knudtson ML; APPROACH Investigators (Alberta Provincial Project for Outcome Assessment in Coronary Heart Disease. Validation of three myocardial jeopardy scores in a population-based cardiac catheterization cohort. Am Heart J. 2001 Aug;142(2):254-61.

129. De Silva K, Morton G, Sicard P, Chong E, Indermuehle A, Clapp B, et al. Prognostic utility of BCIS myocardial jeopardy score for classification of coronary disease burden and completeness of revascularization. The American journal of cardiology. 2013 Jan 15;111(2):172-7.

130. Mohee K, Mynard JP, Dhunnoo G, Davies R, Nithiarasu P, Halcox JP, Obaid DR. Diagnostic performance of virtual fractional flow reserve derived from routine coronary angiography using segmentation free reduced order (1-dimensional) flow modelling. JRSM Cardiovasc Dis. 2020 Nov 5;9:2048004020967578.

131. Perera D, Stables R, Booth J, Thomas M,Redwood S. The Balloon pump-assisted Coronary Intervention Study (BCIS-1): rationale and design. Am Heart J (2009); 158: 910–916. e912

132. Dash H, Johnson RA, Dinsmore RE, Harthorne JW. Cardiomyopathic syndrome due to coronary artery disease. I: Relation to angiographic extentof coronary disease and to remote myocardial infarction. Br Heart J. 1977;39:733–739.

133. Alderman EL, Stadius M. The angiographic definitions of the Bypass Angioplasty Revascularization Investigation. Coron Artery Dis.1992;3:1189–1207.

134. Graham MM, Faris PD, Ghali WA, Galbraith PD, Norris CM, Badry JT,Mitchell LB, Curtis MJ, Knudtson ML; APPROACH Investigators (Alberta Provincial Project for Outcome Assessment in Coronary Heart Disease. Validation of three myocardial jeopardy scores in a population-based cardiac catheterization cohort. Am Heart J. 2001;142:254–261.

135. Leone AM, De Caterina AR, Basile E, et al., Influence of the amount of myocardium subtended by a stenosis on fractional flow reserve, Circ. Cardiovasc. Interv. 6 (1) (2013) 29–36.

136. Baptista J, Arnese M, Roelandt JR, et al. Quantitative coronary angiography in the estimation of the functional significance of coronary stenosis: correlations with dobutamine-atropine stress test, J. Am. Coll. Cardiol. 23 (6) (1994) 1434–1439.

APPENDIX

Chapter 2
A.1. Fragment of spreadsheet

mmHg

Segments

3	AbrName		FullName		Tags	Length	A0	c0	segMon		inType	in1
	in2	in3	segType		outType		out1	out2	out3	Rt	C	
	Angle	DoLoss		A0Taper		ctaper	TaperType		TaperExpk			
	RefineEnds		CollapseP		P0	VEgamma		extP				
1	LCAp	LCAp	SysArt	4	0.17349		800	"0,1"	14	1	0	0
	3	0	Stenosis		0	0	0	0	0	2	1	1
	1	0	0	-1000	-1	1000	0					
2	Stenosis		Stenosis		SysArt	3.49	0.06099		800	"0,1"	0	
	LCAp	0	0	3	0	LCAd	0	0	0	0	0	2
	1	1	1	0	0	-1000	-1	1000	0			
3	LCAd	LCAd	SysArt	2	0.17349		800	"0,1"	0	Stenosis		0
	0	3	6	Bed1	0	0	0	0	0	2	1	1
	1	0	0	-1000	-1	1000	0					

HeartChambers

1	Chamber		Type	V / A	L / R	m1	m2	tau1	tau2	InDelay	
	EresisK		InitVol	Emin	Emax	V0	WallVol				
1	CoroFlow		5	0	0	0	0	0	0	0	0.0E+00
	0	0	0	0	0						

VascularBeds

1	AbrName		FullName		Tags	Resis	ArtComp		VenComp		inType
	outType		extP								
1	Bed1	Bed1	0	100	0.033333333		0	3	4	0	

Parameters

outSettings outVars{root} t

outSettings outVars{tnode} "u,A,p,q,c,Kr"

chamber PrescribedVelocity{1}.path working

chamber PrescribedVelocity{1}.file coroflow

chamber PrescribedVelocity{1}.time time

chamber PrescribedVelocity{1}.Uexpr flow*0.15

inPar HeartPeriod 0.8

inPar dt 2.50E-04

inPar AtrialTimeRatio 0.4

inPar venousP(inPar.SysVen) 6666.1

inPar venousP(2) 11998.98

inPar atrialR(2) 13.3322

inPar doInteraction 0

inPar VentSepConstL 6

inPar VentSepConstR 2

inPar AtrSepConstL 6

inPar AtrSepConstR 2

inPar doPericConstraint 0

inPar PericK 666.61

inPar MyoVol 192.4528302

inPar PericVol 30

inPar PericPhi 40

inPar PericV0 458.0528302

inPar adjustPericV0 0

inPar pzerof(inPar.SysArt) 6666.1

inPar pzerof(inPar.PulmArt) 0

inPar pzerof(inPar.Port) 0

inPar doStarling(inPar.SysArt) 1

inPar doStarling(inPar.PulmArt) 1

inPar doStarling(inPar.Port) 1

inPar InitPres(inPar.SysArt) 106657.6

inPar	InitPres(inPar.SysVen)	6666.1
inPar	InitPres(inPar.PulmArt)	9332.54
inPar	InitPres(inPar.PulmVen)	14265.454
inPar	InitPres(inPar.Port)	11332.37
bed	doResisNL	1
bed	initPcalc	1
bed	enforceRartratio	"[0,0,0,0,0,0,0]"
bed	Rartratio	"[0.3,0.3,0.3,0.3,0.26,0.3,0.3]"
bed	Rvenratio	"[0.3,0.3,0.3,0.3,0.13,0.3,0.3]"
bed	updatePtm0	1
runSettings	windkResisOpt(1)	0
runSettings	windkResisOpt(2)	0
meshPar	taperBoundarySafety	0.3
runSettings	doViscoelasticity	1
chamber	AnnulusInteractionFactor(3)	0.033333333
chamber	AnnulusInteractionFactor(4)	0.05

chamber	nonlinearStiffnessConstant	"[0,0]"
chamber	HeartPeriodRelative	1
runSettings	doWallShearStress	1
runSettings	doConvectiveAlpha	0

Y

0.000216863

#REF!

#REF!

RefCoef	#REF!	RefCoef	Branch A0
	0	3.25	

0.5 1.08

-0.5 9.8

Chapter 3
A.2

	Length of coronary artery/mm	Diameter of stenosed lumen	% area stenosis	Lower FFR	Mid FFR	High FFR
LAD	10	4.5	10	0.99	0.99	0.99
	10	4.0	20	0.99	0.99	0.99
	10	3.5	30	0.99	0.99	0.99
	10	3.0	40	0.99	0.99	0.98
	10	2.5	50	0.98	0.98	0.98
	10	2.0	60	0.97	0.95	0.82
	10	1.5	70	0.89	0.73	NA
	10	1.0	80	0.38	NA	NA
	10	0.5	90	NA	NA	NA
	20	4.5	10	0.99	0.99	0.99
	20	4.0	20	0.99	0.99	0.98
	20	3.5	30	0.99	0.98	0.98
	20	3.0	40	0.98	0.98	0.96
	20	2.5	50	0.97	0.96	0.92
	20	2.0	60	0.94	0.9	0.75
	20	1.5	70	0.81	0.67	0.3
	20	1.0	80	0.33	0.17	NA
	20	0.5	90	NA	NA	NA
	30	4.5	10	0.99	0.99	0.98
	30	4.0	20	0.99	0.99	0.98

	30	3.5	30	0.99	0.98	0.97
	30	3.0	40	0.98	0.97	0.95
	30	2.5	50	0.96	0.95	0.9
	30	2.0	60	0.92	0.87	0.72
	30	1.5	70	0.75	0.6	0.29
	30	1.0	80	0.3	0.16	NA
	30	0.5	90	NA	NA	NA

Table 2.2- Variation of FFR with increasing % area of stenosis and lesion length in LAD.

A.3

Coronary Artery	Length of coronary artery/mm	Diameter of stenosed lumen	% area stenosis	Lower FFR	Mid FFR	High FFR
LCX	10	2.7	10	0.99	0.98	0.97
	10	2.4	20	0.99	0.98	0.97
	10	2.1	30	0.98	0.98	0.96
	10	1.8	40	0.98	0.97	0.95
	10	1.5	50	0.96	0.95	0.9
	10	1.2	60	0.92	0.88	0.7
	10	0.9	70	0.77	0.61	NA
	10	0.6	80	0.29	NA	NA

	10	0.3	90	NA	NA	NA
	20	2.7	10	0.99	0.98	0.97
	20	2.4	20	0.98	0.98	0.96
	20	2.1	30	0.98	0.97	0.94
	20	1.8	40	0.96	0.95	0.91
	20	1.5	50	0.93	0.9	0.83
	20	1.2	60	0.86	0.79	0.6
	20	0.9	70	0.64	0.5	0.25
	20	0.6	80	NA	NA	NA
	20	0.3	90	NA	NA	NA
	30	2.7	10	0.98	0.98	0.96
	30	2.4	20	0.98	0.97	0.95
	30	2.1	30	0.97	0.96	0.93
	30	1.8	40	0.95	0.93	0.88
	30	1.5	50	0.91	0.87	0.78
	30	1.2	60	0.81	0.73	0.54
	30	0.9	70	0.56	0.43	0.22
	30	0.6	80	0.2	0.12	NA
	30	0.3	90	NA	NA	NA

Table 2.3- Variation of FFR with increasing % area of stenosis and lesion length in LCX.

A.4

Coronary Artery	Length of coronary artery/mm	Diameter of stenosed lumen	% area stenosis	Lower FFR	Mid FFR	High FFR
LMS	10	5.4	10	1	1	0.99
	10	4.8	20	0.99	0.99	0.99
	10	4.2	30	0.99	0.99	0.99
	10	3.6	40	0.99	0.99	0.98
	10	3	50	0.99	0.98	0.97
	10	2.4	60	0.98	0.96	0.87
	10	1.8	70	0.92	0.77	0.31
	10	1.5	80	0.4	NA	NA
	10	1.2	90	NA	NA	NA
	20	5.4	10	1	0.99	0.99
	20	4.8	20	0.99	0.99	0.99
	20	4.2	30	0.99	0.99	0.98
	20	3.6	40	0.99	0.98	0.97
	20	3	50	0.98	0.97	0.94
	20	2.4	60	0.96	0.93	0.81
	20	1.8	70	0.85	0.7	0.32
	20	1.5	80	0.37	NA	NA
	20	1.2	90	NA	NA	NA
	30	5.4	10	0.99	0.99	0.99
	30	4.8	20	0.99	0.99	0.98
	30	4.2	30	0.99	0.99	0.98

	30	3.6	40	0.98	0.98	0.96
	30	3	50	0.97	0.96	0.93
	30	2.4	60	0.94	0.91	0.78
	30	1.8	70	0.81	0.66	0.3
	30	1.5	80	0.34	0.17	NA
	30	1.2	90	NA	NA	NA

Table 2.4- Variation of FFR with increasing % area of stenosis and lesion length in LMS.

A.5

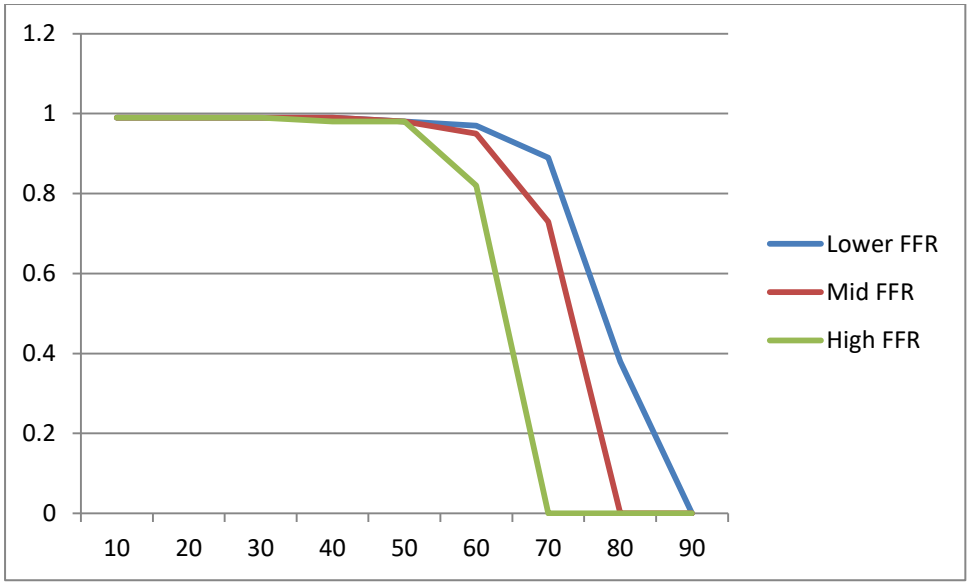

Figure 2.6- Variation of FFR with increasing % area of stenosis with lesion length 10mm in LAD.

A.6

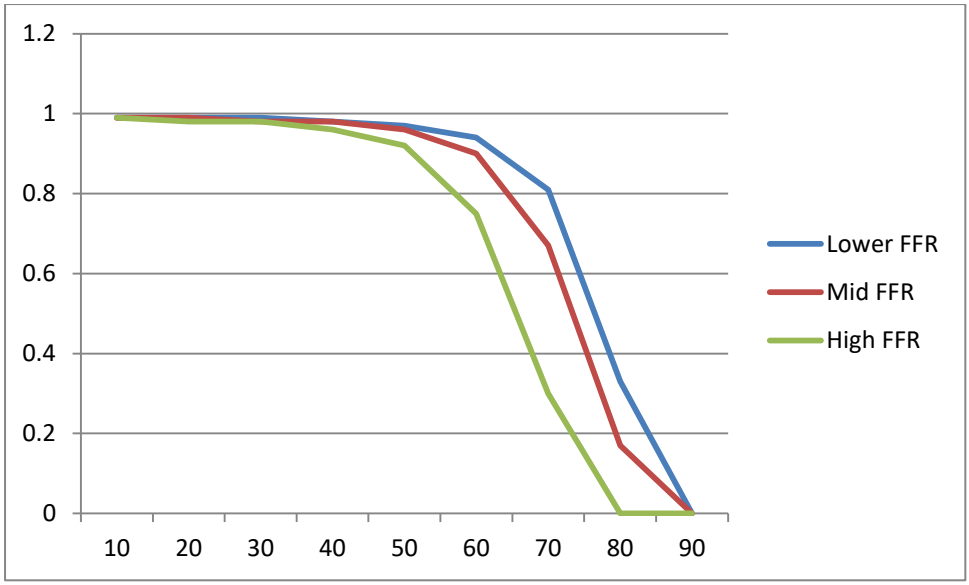

Figure 2.7- Variation of FFR with increasing % area of stenosis with lesion length 20mm in LAD.

A.7

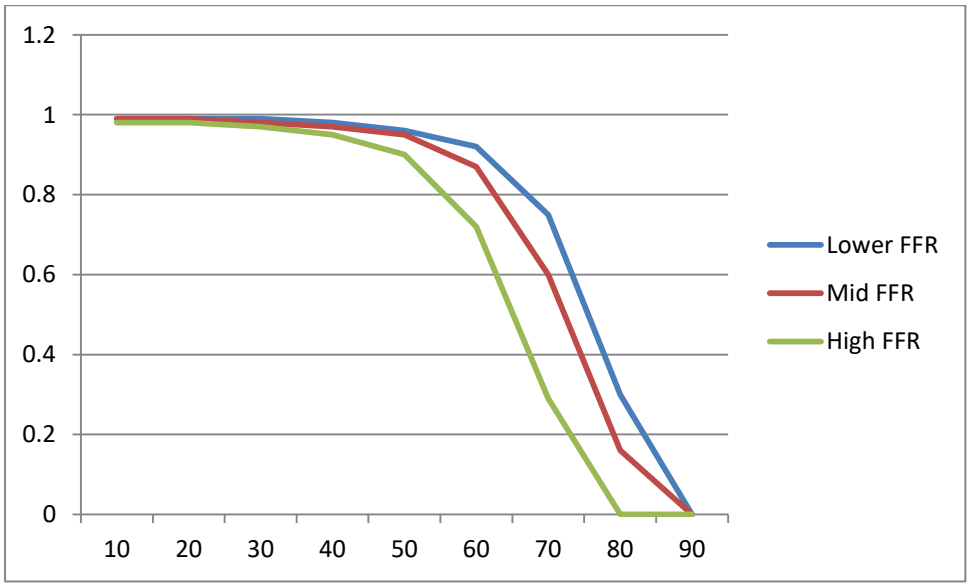

Figure 2.8- Variation of FFR with increasing % area of stenosis with lesion length 30mm in LAD.

A.8

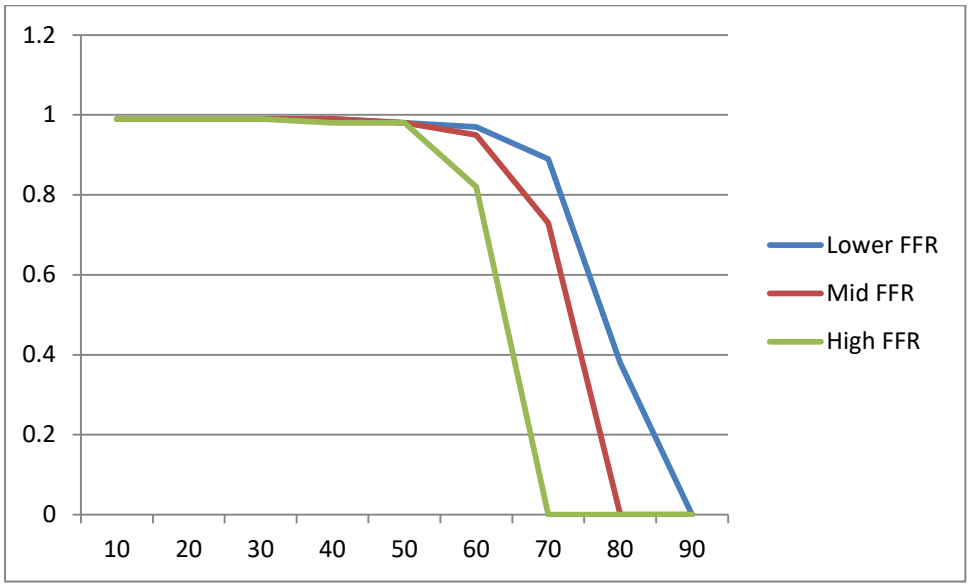

Figure 2.9- Variation of FFR with increasing % area of stenosis with lesion length 10mm in LCX.

A.9

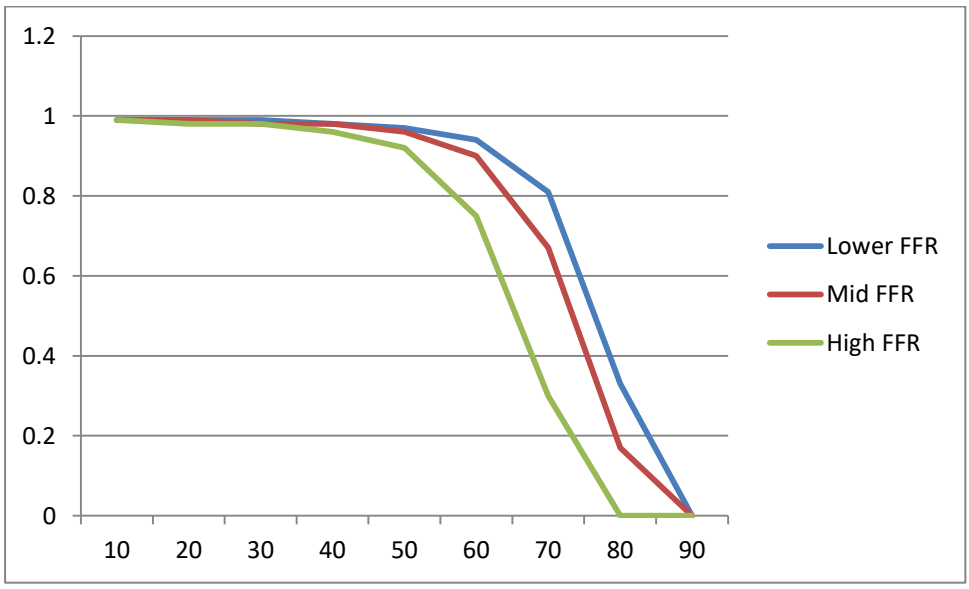

Figure 2.10- Variation of FFR with increasing % area of stenosis with lesion length 20mm in LCX

A.10

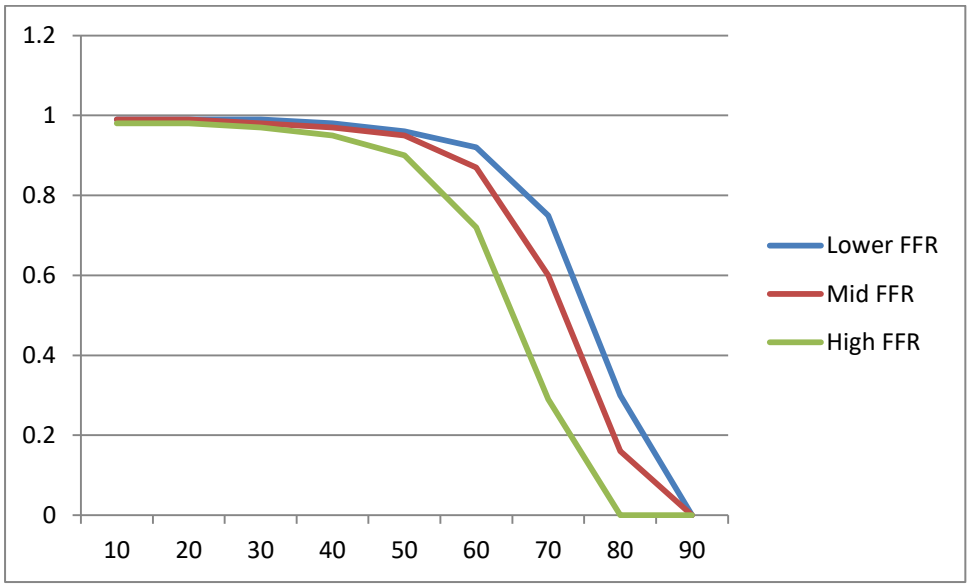

Figure 2.11- Variation of FFR with increasing % area of stenosis with lesion length 30mm in LCX.

A.11

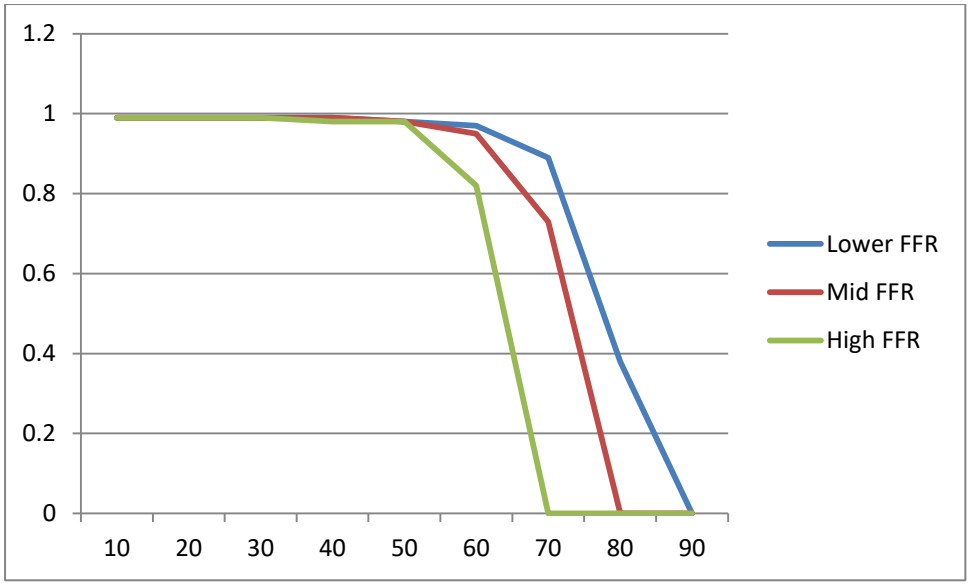

Figure 2.12- Variation of FFR with increasing % area of stenosis with lesion length 10mm in LMS.

A.12

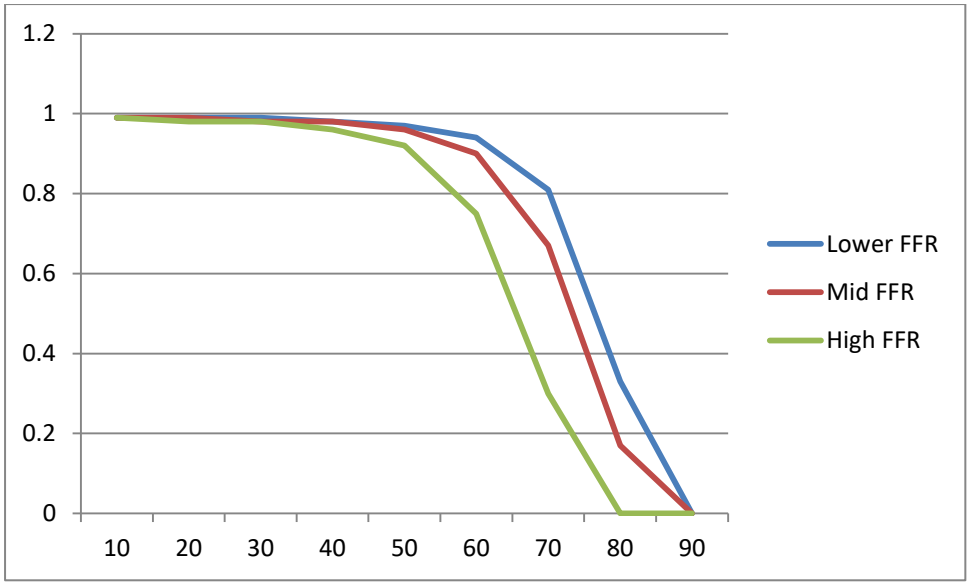

Figure 2.13- Variation of FFR with increasing % area of stenosis with lesion length 20mm in LMS.

A.13

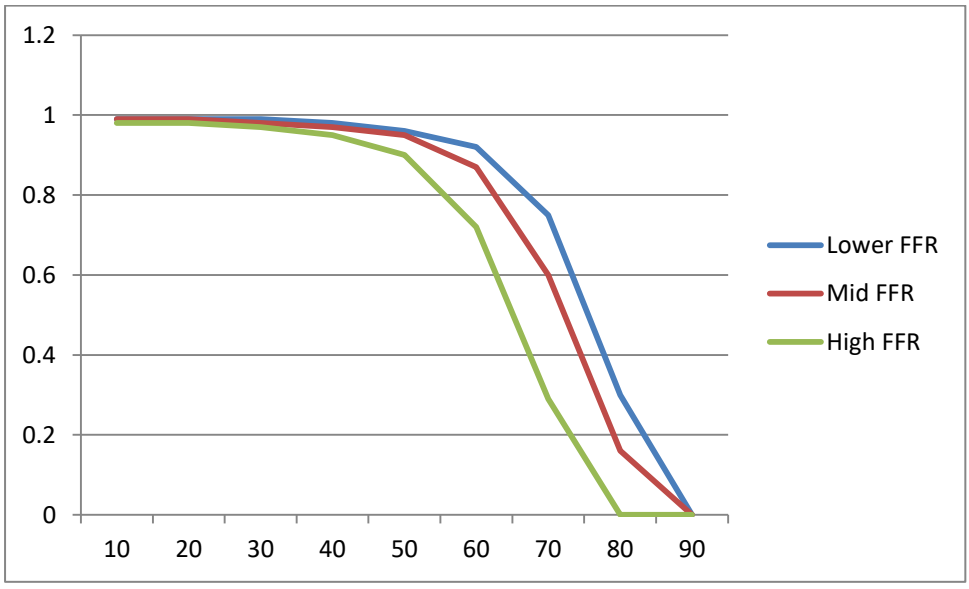

Figure 2.14- Variation of FFR with increasing % area of stenosis with lesion length 30mm in LMS.

Suggested Layout of Declaration/Statements page

DECLARATION

This work has not previously been accepted in substance for any degree and is not being concurrently submitted in candidature for any degree.

Signed .K.Mohee..... (candidate)

Date .15/6/22.....

STATEMENT 1

This thesis is the result of my own investigations, except where otherwise stated. Where correction services have been used, the extent and nature of the correction is clearly marked in a footnote(s).

Other sources are acknowledged by footnotes giving explicit references. A bibliography is appended.

Signed..K.Mohee..... (candidate)

Date ..15/6/22.....

STATEMENT 2

I hereby give consent for my thesis, if accepted, to be available for photocopying and for inter-library loan, and for the title and summary to be made available to outside organisations.

Signed K.Mohee..... (candidate)

Date ..15/6/22.....

NB: *Candidates on whose behalf a bar on access has been approved by the University (see Note 7), should use the following version of Statement 2:*

I hereby give consent for my thesis, if accepted, to be available for photocopying and for inter-library loans **after expiry of a bar on access approved by the Swansea University.**

Signed .K.Mohee..... (candidate)

Date .....15/6/22.....